THE ELECTROMAGNETIC PROPERTIES OF OBSTACLE-TYPE DIELECTRICS WITH REGULAR AND IRREGULAR STRUCTURES

bу

H. J. Peppiatt

A thesis submitted in partial fulfilment of the requirements for the degree of Doctor of Philosophy to the raculty of Graduate Studies and Research, McGill University.

Eaton Electronics Research Laboratory,

McGill University.

August 1953.

TABLE OF CONTENTS

		Pa	ige No.
	ABSTRACT		i
	ACKNOWLEDGEMENTS	•	ii
	LIST OF SYMBOLS		ii i
1	INTRODUCTION		1
2	THEORY OF ARTIFICIAL DIELECTRICS	•	5
	(2:1) Types of Artificial Dielectrics	•	5
	Dielectrics		8 12
	(2:3) Interaction Theories of Artificial Dielectri	CB	12
3	EXPERIMENTAL MEASUREMENTS	•	20
	(3:1) Description of Apparatus		20
	(3:2) Propagation Constants and Wave Impedances in Rectangular Waveguides		23
	(3:3) Theory of the Short circuit-Open circuit measurements	•	33
	Homogeneous Isotropic Dielectrics Homogeneous Anisotropic Dielectrics		37 40
4	EXPERIMENTAL ACCURACY	•	47
	(4:1) Experimental Errors in the Short circuit-Ope circuit Measurements		47
	(4:2) Accuracy of Samples		55 55
5	EXPERIMENTAL RESULTS	•	59
	(5:1) Alumirum and Copper Powders in Wax (5:2) Aluminum Disc Array in Wax (5:3) Aluminum Disc Arrays in Polystyrene	•	59 63 68
6	CONCLUSIONS	•	84
	APPENDIX A		87
	APPENDIX B		92
	BIBLIOGRAPHY		95

Abstract

It has been showr quantitatively that the diamagnetic effect of large flake-like metal powder dielectrics is smaller than predicted by simple theories. Measurements were made on regular arrays of aluminum foil discs of uniform circular contour in an attempt to isolate the main causes of this effect. To do this the theory of the Short circuit - Open circuit waveguide technique was enlarged in scope to treat certain media of electric and magnetic anisotropy. Experimental values of the permeability, dielectric constant and loss tangents of the disc arrays were obtained. It was found that the metal powder dielectrics exhibit small diamagnetic effects because of the interaction between particles of approximately circular contours and because of the small magnetic polarizabilities of the more elongated particles. A practical procedure for estimating the experimental errors in the measured electric and magnetic parameters has been given.

ACKNOWLEDGEMENTS

The writer is pleased to thank Professor G. A. Woonton for his constant advice and encouragement. Frequent discussions with Dr. H. E. J. Neugebauer concerning the interpretation of the experimental results are also appreciated. Drs. G. Bekefi, D. C. Hogg, and E. I. Vogan contributed to many discussions on the subject. The writer is also indebted to Mrs. H. J. Peppiatt for her assistance in the preparation of the thesis.

During the summer months financial assistance was received from the Electronics Research Directorate of the Air Force Cambridge Research Center.

LIST OF SYMBOLS

^Åa = rectangular waveguide dimension.

= real part of Yid.

A, A_1 , A_2 = symbols introduced for convenience in the discussion of the theory of the measurements (see equation (3:3:8)).

 A_x , A_y , A_z = lattice structure correction terms.

tb = rectangular waveguide dimension.

= imaginary part of γ_i d

 \vec{B} = magnetic induction.

B, B_1 , B_2 = symbols introduced for convenience in the discussion of the theory of the measurements (see equation (3:3:7)).

c = the velocity of electromagnetic waves in free space.

d = length of the dielectric sample.

 \vec{D} = displacement vector.

 \vec{E} = electric intensity.

 $E_{O} =$ inverse standing wave ratio.

f = frequency.

 \vec{F} = vector potential.

H = magnetic intensity.

I(pq), I[pq] = waveguide currents analagous to ordinary transmission
line currents.

 $j = \sqrt{-1}$.

 k_e = dielectric constant.

 $\mathbf{k}_{\mathtt{m}}$ = nermeability or relative permeability.

kd = dielectric constant of the supporting medium.

 $k_e^{"}$ = dielectric constant of the obstacles.

K = wave number vector.

L = separation between the plates of a waveguide medium.

 \vec{N} = magnetization vector.

n = refractive index.

N = number of particles per unit volume.

p = electric dipole moment.

P = electric polarization.

R = radius of circular disc.

S = spacing between discs (see Figure 7).

 S^{I} , S^{II} , T^{I} , T^{II} = numerical values of quantities obtained from the measured values of the positions of the first minima and the inverse standing wave ratios.

 $T_{(pq)}(xy)$, $T_{pqq}(xy) = T$ functions used by Schelkunoff²⁰.

IT, VT = transfer coefficients introduced to represent coupling between the propagation modes of waveguides.

U = scalar potential.

V' = scalar potential.

X = distance from the sample to the first voltage minimum.

Y(pq)(st), etc, = transfer admittances introduced to represent coupling between the propagation modes of waveguides.

 $Z_{(pq)(st)}$, etc., = transfer impedances introduced to represent coupling between the propagation modes of waveguides.

 Z_{ki} = characteristic wave impedance in a dielectric filled guide.

Z = characteristic wave impedance in an empty guide.

 Z_{kil} = see page 33.

 Z_{ki2} = see page 33.

 $Z_{ki[10]}$ = characteristic wave impedance for the TE [10] mode.

 Z_t = termination impedance.

 $\alpha_{\rm e}$ = electric polarizability.

 $a_m = magnetic polarizability.$

 β_e , β_m = "apparent" electric and magnetic polarizabilities.

 β_{0} = propagation constant in an empty guide.

 γ_i = propagation constant in a dielectric filled guide.

Yo = propagation constant in an empty guide.

 Y_{i1} , Y_{i2} = see page 33.

AX = distance between the two twice minimum power positions in the standing wave pattern.

 λ = free space wavelength.

 λ_c = cut-off wavelength.

 $\lambda_{\rm gi}$, $\lambda_{\rm go}$ = guide wavelength in dielectric filled and empty guide.

 γ = stream function.

II = stream function.

 $\chi_{\text{(ma)}}$ = eigenvalues corresponding to the T functions.

 ω = angular frequency.

i = complex permeability.

 θ , θ_1 , θ_2 = symbols introduced for convenience in the discussion of the theory of the measurements (see equation (3:3:8)).

 \emptyset , \emptyset_1 , \emptyset_2 = symbols introduced for convenience in the discussion of the theory of the measurements (see equation (3:3:7)).

 $tanb_{e}$, $tanb_{m}$ = electric and magnetic loss tangents.

. Itanb = the total loss tangent.

A. Rather than deviate from starlard notations, in a few cases a symbol is used to represent more than one quantity. No confusion should arise since the particular representations are made clear in the cortext.

Introduction

Ever since the realization that optical techniques might lead to important developments when applied to the microwave region of the electromagnetic spectrum, the search for a low loss, light weight dielectric has been intensive. The dimensions of lenses, prisms, etc., at these wavelengths must be large in order to avoid diffraction effects and to produce the required phase change. For example, a typical lens at a wavelength of 3.2 cms. with a refractive index of 1.5 would have an aperture diameter of about 3 meters and a thickness of about 20 cms. If it were made of glass or polystyrene its large weight would present many difficulties in most practical applications. To avoid these difficulties W.E.Kock^{1,2} developed two types of "artificial dielectrics". The first was made of parallel metallic strips separated from one another by a distance L. The focusing effect arose by virtue of the high phase velocity between the plates which act as waveguides. The refractive index is given approximately by the relation

$$n = \sqrt{1 - (c/2fL)^2}$$

where f is the frequency and c is the velocity of light in free space. This shows that the dielectric exhibits dispersion to a marked degree, a property undesirable for wideband applications. The second dielectric consisted of a regular array of metallic objects supported in space by insulating material. Each object polarizes, both electrically and magnetically, in an electromagnetic field. A simple analysis of such an array shows that the refractive index is given by the relation

$$n = \sqrt{(1 + \alpha_{e}N) (1 + \alpha_{m}N)}$$

where N is the number of objects per unit volume and α_m , α_e are the magnetic and electric polarizabilities respectively. Here, again, diffraction effects occur, but only when the spacing between the objects is of the order

of a wavelength. Also, resonance effects are present if the dimensions of the object are comparable with the wavelength. The construction of a lens free from such effects at the shorter micro-wavelengths would be impractical.

J.A.Carruthers³ has recently developed an artificial dielectric material consisting of small aluminum particles randomly embedded in a light weight insulating medium. Such a material should not exhibit the troublesome diffraction and resonance effects of the dielectrics of Kock's. E.L.Vogan⁴ has investigated the properties of these Aluminum Flake Dielectrics in a waveguide by the Short circuit - Open circuit method developed by W.B.Westphal⁵. Since he found that the diamagnetic effect was small, most of his investigation was concerned with the electric properties. Carruthers has attempted to explain the small diamagnetic effect from a consideration of the finite conductivity of the particles, all previous theories having been based on the assumption of infinite conductivity. He concluded that aluminum flake particles of thicknesses of the order of skin depth or less would not exhibit diamagnetism.

The work which this thesis reports was done principally to gain a better understanding of the magnetic properties of the dielectric. First, an investigation of thick aluminum and copper particles embedded in a wax medium was carried out to determine whether Carruthers' theory gives a complete explanation of the small diamagnetic effects. A simple but effective method of making homogeneous samples was devised which produced consistent and more accurate values of the electric and magnetic parameters.

A quantitative interpretation of measurements of randomly positioned and oriented particles with sizes and shapes which vary over wide ranges is obviously not possible. For this reason a series of measurements on regular arrays of aluminum discs of uniform size was necessary. To make the measurements, the Short circuit - Open circuit waveguide method, which considered only isotropic media, was extended to apply to anisotropic electric and magnetic media by the use of Schelkunoff's Generalized Telegraphists Equations¹⁹. Because of errors associated with the Interface Problem, measurements for two orientations of the anisotropic medium are required for the accurate determination of the complex permittivities and permeabilities. The theory of this measurement has not previously appeared in the literature.

The measurements of the thick aluminum and copper particles in a wax medium indicate that the diamagnetic effect is still small. Hence, Carruthers' explanation of the absence of the diamagnetic effect which applies only to thin particles is not complete. The simple theoretical expressions for kekm, ke and km acree with the experimental values for the aluminum disc array samples when the discs are not too close to one another. From this it is concluded that the expressions for the polarizabilities are correct, that is, that they are not modified by the effect of the finite conductivity of the obstacles. However, when the discs are closely packed, the experimental values deviate radically from theory, the values of $k_{I\!I\!I}$ being closer to unity than predicted. Hence, it appears that a complete theoretical explanation of the small magnetic effect will result from a rigorous consideration of the interaction between the obstacles. Recently C.Flammer 17 has calculated the propagation constant in an infinite array of metallic objects by an extension of the Seitz-Slater cellular method used in Solid State Theory. The result is not expressible in analytic form and. as yet, no numerical results have been reported for comparison with the values obtained in this work.

The expressions for the electric and magnetic parameters in terms of the positions of the first minima and the voltage standing wave ratios obtained from the Short circuit-Open circuit theory have been revised, thus resulting in a considerable reduction in the numerical calculations. Also, because of these revisions, comparatively simple expressions for the errors involved are obtained.

Chapter 2 Theory of Artificial Dielectrics

2:1 Types of Artificial Dielectrics

at the present time, they may be classed in either one of two groups according to the manner in which the phase change is achieved. One of these groups may be called the waveguide or metal plate dielectrics. They were developed independently by Kock, Rust and Stuetzer^{1,6,7}. It is well known that when an electromagnetic wave passes between two parallel metal plates spaced a distance, L, apart, the phase velocity is increased to the value

$$v = c/\sqrt{1 - (c/2Lf)^2}$$

where c is the phase velocity in free space and f is the frequency, thus resulting in a refractive index given by

$$n = \sqrt{1 - (c/2Lf)^2}$$
.

In a lens these metal plates are made to suitable contours and are equally spaced side by side. Such lenses are lighter and less expensive than those of glass or polystyrene with the same properties. The principle disadvantage of lenses made of this medium arises from the fact that the refractive index depends explicitly on the frequency. Kock has observed that lenses having large apertures (in wavelengths) have very serious bandwidth limitations. Also, the lens action is restricted to one polarization.

In 1948 Kock² proposed artificial dielectric materials which did not suffer from the serious limitations of the waveguide media. It is this group of dielectrics which will be discussed in the rest of this thesis. These materials consist of metallic obstacles supported in a regular three dimensional array in an attempt to simulate the crystalline lattice of ordinary dielectrics. Each particle becomes polarized in the presence of an electromagnetic wave, the effect of the whole array thus resulting in a phase delay and a refractive

 V_{\perp}

index greater than one. The analogy with the polarization of an atom in a crystalline lattice is not nearly complete however, since there is in general a comparatively large diamagnetic polarizability associated with the metallic obstacles which is absent in ordinary dielectrics.

Such obstacle type dielectrics have been constructed using various shaped objects supported in lattice structures in many different ways. Polystyrene foam has been used extensively as a supporting medium since it is a light weight material with negligible loss. Spherical obstacles have been used, but there is an upper limit to the value of n because of space requirements and their large diamagnetic effect. Corkum8 shows that the theoretical limit is 1.273 and states that the practical value obtained is much less. Susskind has pointed out that dielectric spheres of high dielectric constant also produce a delay effect similar to that of the metallic spheres and that the refractive index might be made larger since the diamagnetic effect is absent. However, materials of high dielectric constant are usually lossy and the attenuation in such an array would prohibit their use. Disc shaped metallic obstacles also have been used extensively. Their shape is such that the magnetic polarizability is negligible when the disc face is oriented parallel to the magnetic field. There appears to be no upper limit to the refractive index in this case since the number of discs per unit volume can be very large. When used as a lens, however, the disc array displays anisotropic effects since it is not always possible to have the magnetic vector parallel to the face of the disc. However, Estrin10 has shown that it might be possible to design a lens corrected for these effects.

The obstacle type dielectricshave many other attractive features which make them more suitable as lens materials. For example, an obstacle

type lens can be matched to free space by reducing the size of the obstacles at the surfaces, thus forming a quarter wave matching device. Also, the refractive index may be made a function of position by varying the size of the obstacles or by a continuous change of the lattice dimensions.

There are two major requirements that are imposed or the lattice medium which make their construction impractical for use at the shorter microwavelengths. First, the lattice spacing must be much less than a wavelength to avoid diffraction effects similar to those which occur in ordinary dielectrics at K-ray wavelengths. The other requirement places a limitation of the size of the chatacles with respect to the wavelength. Any metallic object has associated with it natural modes of electromagnetic oscillation with frequencies which are related to the size and shape of the object. Hence, anomalous dispersion occurs when the frequency of the applied electromagnetic wave in the one of the resonance frequencies. The wavelength associated with the lowest potural frequency is of the order of the dimensions of the obstacle, in which case the dispersion is not noticable when the wavelength of the applied wave is much greater than the obstacle dimensions.

Because of these restrictions it is doubtful that a lens could be built for wavelengths below 7.5 cms. The weight and the number of obstacles would be large and the mechanical difficulties in placing them in a regular array would be great.

Constitutes suggested that the obstacles need not necessarily be placed in a lattice and that to avoid diffraction and anomalous dispersion the obstacles could be small metallic particles such as those used in paints Measurements made by Vogan⁴ on flake-like aluminum particles embedded in wax indicate that high values of refractive index can be obtained. Although the dielectric constant of these randomly oriented particles which resembled discs more than any other simple geometrical figure, increased almost linearly

with the mass of the particles per unit volume, the permeability decreased very little from unity. Actually, he did not measure any permeabilities less than 0.900. Wax, of course, cannot be used as a supporting medium for a lens. A light weight artificial dielectric was made by mixing aluminum powder in an alkyd resin foam with some success. However, the resultant dielectric was slightly anisotropic and the losses were excessive. At the present time research workers at Dow Chemical Company are attempting to place the aluminum in polystyrene foam to lower the losses inherent in the supporting medium.

2:2 Simple Theory of Obstacle Type Artificial Dielectrics

The simple theory of obstacle type artificial dielectrics is based on the assumption that there is no electromagnetic interaction between the obstacles, hence it will be referred to as the No-interaction Theory. It is difficult to say at what lattice spacing this assumption is valid. However, a simple calculation shows that the dipole field set up by a metallic disc in an applied electric field is as little as one-twentieth of the applied field at a distance of twice its own radius. At distances smaller than this the dipole fields increase rapidly and the interaction This No-interaction theory also requires is probably not negligible. that the obstacle size is much less than the wavelength. Only in this case do k_e and k_m have any meaning either theoretically or operationally. For example, suppose the dielectric constant of an array of obstacles of dimensions greater than a wavelength is to be measured at 9370 mcps. order that the measurement may be made, the dimensions of the apparatus. for example plane parallel condenser plates, must be much less than a wavelength, in which case the comparatively large size of the obstacles

would make the measurement impossible for mechanical reasons. However, the refractive index does have meaning even though none can be associated with k_e or k_m , and it could be determined by measuring the phase delay by the free space method. Nevertheless, this is not an important restriction on the theory since the obstacle size of the dielectrics of interest must be much less than a wavelength to avoid resonance.

According to the No-interaction assumption, each obstacle in the array polarizes under the influence of the fields, the polarizations being linearly dependent on the applied fields. In the electric case \vec{P} , the polarization is given by the relation

$$\vec{P} = \epsilon_0 \alpha_e N \vec{E}$$

where $\vec{\mathbf{E}}$ is the macroscopic field, N is the number of obstacles per unit volume and $\alpha_{\mathbf{e}}$ is a constant with dimensions of volume which depends on the shape and size of the obstacle. $\alpha_{\mathbf{e}}$ is defined by the relation

$$\vec{p} = \epsilon_{\mathbf{a}} \alpha_{\mathbf{e}} \vec{\mathbf{E}}_{\mathbf{a}}$$

where \vec{p} is the dipole moment of the obstacle when placed in a uniform applied field, \vec{E}_a . α_e is called the polarizability of the obstacle and is usually obtained by solving Laplaces Equation subject to the boundary conditions at the surface of the obstacle and at large distances where the field is uniform. This static solution does not differ from the quasistatic one if the conductivity of the object is infinite. α_e is 16/3 R³ for a thin circular disc of radius R if the electric vector lies in the plane of the disc and zero if it is perpendicular. This result can also be obtained by examining the electric dipole radiation scattered by the disc for wavelengths greater than its dimensions. If the obstacle is embedded in a dielectric, the new expression for the polarizability is simply the polarizability of the object in free space multiplied by k_e , the dielectric sonstant of the

supporting medium. In this case the polarization becomes

$$\vec{P} = \epsilon k_e \alpha_e N \vec{E}$$

Using these expressions for P along with the definition of the displacement, the dielectric constant is

$$k_e = 1 + \alpha_e N$$

when the obstacles are supported in a medium of dielectric constant unity and

$$k_e = k_e'(1 + \alpha_e N)$$

for a dielectric medium. This latter modification, although not obvious, has been justified in a recent report by H.E.J.Neugebauer 11.

Satisfactory theoretical explanations of magnetic effects in ordinary magnetic materials are usually based on a microscopic theory of matter, hence on Quantum Mechanics. Diamagnetic effects in such materials are extremely small and very accurate experimental equipment must be used to measure permeabilities different from one. However, the diamagnetism of obstacle type dielectrics has its origin in current loops of macroscopic size and the corresponding permeabilities might be much less than one. This is a decided disadvantage in the delay-type media. If an array of obstacles is placed in a magnetic field varying sinusoidally with the time and if the interaction between obstacles can be neglected, the No-interaction expression for the magnetization is

$$\vec{M} = c_m N \vec{H}$$

where \vec{H} is the macroscopic magnetic intensity, N is the number of obstacles per unit volume and α_m is the magnetic polarizability. This polarizability is defined by

$$\vec{m} = \alpha_m \vec{H}_a$$

where \vec{m} is the magnetic moment of one such obstacle placed in a uniform magnetic field, $\vec{H}_a = \vec{H}_{ao}$ sinct. Again, α_m depends on the size and shape of the obstacle and is usually obtained by solving a magnetic boundary value problem. In this solution it is assumed that the frequency is large

so that the skin depth is small and the field within the metallic obstacle is zero. Even an array of ferromagnetic obstacles will exhibit diamagnetism if the skin depth is less than the dimension of a domain. Because of the discontinuity in the tangential component of H at the boundary of the obstacle, large currents flow along the surface. It is these surface currents which produce the diamagnetic effect and the polarizability is obtained by integrating the product of the loop current and loop area over the complete surface. Corkum⁸ has derived the polarizability for a sphere in a recent paper in which the physical situation was made clear. The polarizability for a circular disc of radius R was found by Estrin 12 to be -8/3 R3 when the disc is perpendicular to the magnetic field and zero when parallel. He considered an oblate spheroidal metallic obstacle and by a suitable limiting process obtained an expression for the currents on the surface of a disc. From this the expression for the polarizability was evident. All derivations were based on the assumption that the obstacles are perfectly conducting, although Estrin suggests a means of extending his solution to the case of finite conductivity.

If the expression for the magnetization is substituted into the relation $\vec{B} = \mu_0(\vec{H} + \vec{M})$, k_m is given by the relation

$$k_m = 1 + \alpha_m N_{\bullet}$$

The refractive index, n, is obtained by taking the square root of the product of the dielectric constant and the permeability, thus

$$n = \sqrt{1 + \alpha_{e} N (1 + \alpha_{m} N)}$$

which must be modified in the usual way to give

$$n = \sqrt{k_e!(1 + \alpha_eN) (1 + \alpha_mN)}$$

for a dielectric supporting medium.

It was mentioned that circular disc obstacles have different properties for different orientations with respect to the fields. Thus both the dielectric constant and the relative permeability of a disc array may be represented as

2:3 - 12 -

tensors with principle axes which coincide with the coordinate axes. Such an array is depicted schematically in Figure 1a with the principle axes drawn parallel to the coordinate axes. If an electric field, $\mathbf{E}_{\mathbf{x}}$, is applied in the x-direction, a displacement of charge is not possible and hence $\mathbf{D}_{\mathbf{x}} = \boldsymbol{\epsilon}_{\mathbf{0}} \mathbf{E}_{\mathbf{x}}$. An electric field applied in the y and z direction results in similar displacements of charge with a result that $\mathbf{D}_{\mathbf{y}} = \boldsymbol{\epsilon} \mathbf{E}_{\mathbf{y}}$, $\mathbf{D}_{\mathbf{z}} = \boldsymbol{\epsilon} \mathbf{E}_{\mathbf{z}}$. Hence, it is not possible to describe the electric properties of the dielectric by means of a single constant but a tensor quantity

$$(\epsilon) = \begin{pmatrix} \epsilon_0 & 0 & 0 \\ 0 & \epsilon & 0 \\ 0 & 0 & \epsilon \end{pmatrix}$$

must be used. In a similar way it may be seen that the medium is anisotropic in its magnetic properties and the permeability tensor is

$$(\mu) = \begin{pmatrix} \mu & 0 & 0 \\ 0 & \mu_0 & 0 \\ 0 & 0 & \mu_0 \end{pmatrix}$$

If the discs are randomly oriented, the medium becomes isotropic and it can be shown that the refractive index is given by the relation^{3,4}

can be shown that the refractive index is given by the relation^{3,4}

$$n = \sqrt{(1 + \frac{2N\alpha_e}{3}) + (1 + \frac{N\alpha_e}{3})} \qquad ...(2:2:1)$$

which is modified in the usual way when ki is not one.

2:3 Interaction Theories of Artificial Dielectrics

Examined closely it will become evident that a medium of high refractive index is not possible unless the number of obstacles per unit volume is large. However, if this is so, the expressions for n are no longer valid and theories which attempt to include the interaction must be examined. In this section the physical basis and limitations of the existing theories will be discussed in detail with special emphasis on those which can be applied to disc shaped obstacles.

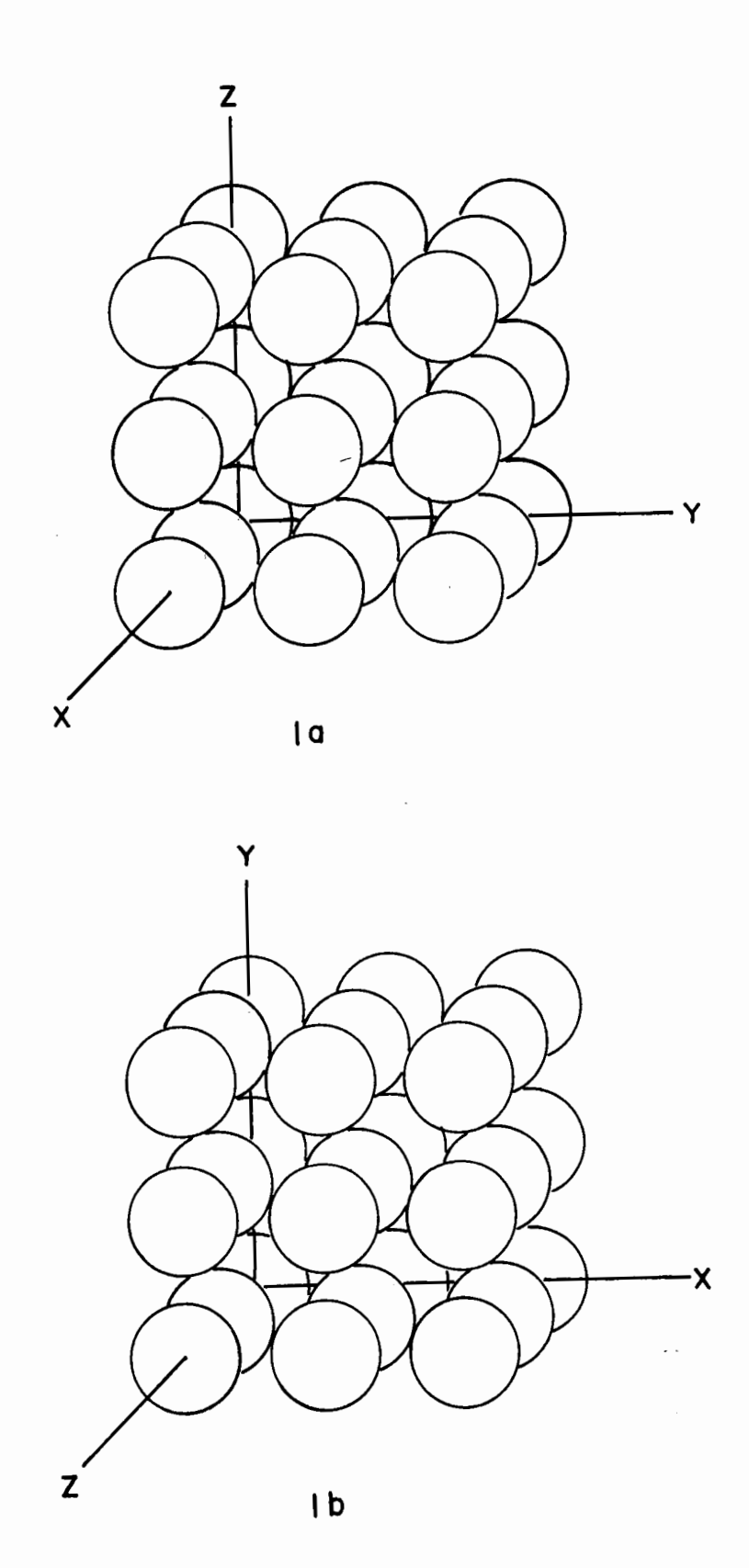


Figure 1. Rectangular Lattice Arrays of Circular Disc Obstacles

Perhaps the most useful of such theories at the present time is the extension of Lorentz's method of treatment of dipolar interaction. Lorentz was aware that there are two types of interaction forces between atoms or molecules in an ordinary dielectric. The van de Waal, chemical bonds and others which are short range saturated forces form one group which must be explained by the Quantum Theory. Because of their saturation properties and short range, only the interaction between nearest neighbouring atoms is considered. The other type of forces is the long range dipole-dipole interaction forces. Such forces have no saturation properties and the field at any one atom is influenced by all other atoms or molecules.

In his theory, Lorentz neglected the short range interaction forces and proceeded to calculate the dipole interaction in an ingenious way. He sought an expression for the field acting on one particular dipole, which he called the local field, $\vec{E}_{_{\! I}}$. This field was considered to be made up of three separate fields by imagining a spherical region about the dipole in question. The radius of the sphere is such that the medium outside appeared, electrically speaking, to be a continuous medium rather than an array of dipoles. The three contributions to the field at the center are, E, the macroscopic field; Es, the field set up by the polarized charge at the surface of the sphere and \mathbb{Z}_d , the field due to the dipoles inside the sphere. If the dielectric is between two parallel plates, [E] is $V/d_{\mathfrak{p}}$ where V is the applied voltage and d_n is the separation of the plates. \overline{E}_s can be calculated by solving Leplace's equation for the field inside & spherical cavity in a homogeneous isotropic dielectric with a uniform applied This is a simple boundary value problem which gives $\vec{E}_s = -\vec{P}/3\xi_0$ where \vec{p} is the polarization. The third term is the sum of the field of the dipoles in the lattice array which lie inside the sphere. Fortunately, if the (2:3) - 15 -

lattice is spherically symmetric it can be shown that \vec{E}_d is zero, a result which is almost intuitively obvious. By using the relations $\vec{E}_L = \vec{E} - \vec{P}/3 \epsilon_0, \ \vec{P} = \epsilon_0 N\alpha_e \vec{E}_L, \ \text{and} \ \vec{D} = \epsilon_0 k_e \vec{E}, \ \text{the dielectric constant becomes}$

$$k_e = 1 + \frac{\alpha_e N}{1 - \frac{\alpha_e N}{3}}$$

which, when written as

$$\frac{k_{e} - 1}{k_{e} + 2} = \frac{N\alpha_{e}}{3} \qquad ...(2:3:1)$$

is known as the Clausius-Mossotti equation. This expression describes the dielectric properties of gaseous and some liquid dielectrics but it cannot apply to solid dielectrics. This is due to the neglect of the short range forces.

The above analysis would seem to apply to artificial dielectrics without revision, especially since there are no short range forces, the only type of interaction being of electrical origin. If the obstacles are effectively supported in free space, the expression for n becomes

$$n = \sqrt{\left(1 + \frac{\alpha_e N}{1 - \alpha_e N}\right) \left(1 + \frac{\alpha_m N}{1 - \alpha_m N}\right)} \qquad \dots (2:3:2)$$

which, again, is multiplied by keto account for the surrounding medium.

Because of the assumptions in the derivation of the Clausius-Mossotti equation, it appears that the equation cannot be applied to a lattice structure which is not spherical or arrays which exhibit anisotropic properties such as a disc array. However, H.E.J.Neugebauer 13 has shown that this equation still applies if the expression for the polarizability is replaced by an "apparent" polarizability, β_e or β_m , which includes the effect of the lattice structure and the anisotropy. For example, in the electric case, k_{eX} , the dielectric constant along a principle axes of a disc array is given by

$$\frac{k_{ex}-1}{k_{ex}+2} = \frac{N\beta_{ex}}{3}$$

where $1/\beta_{\rm ex}=A_{\rm x}+1/\alpha_{\rm ex}$, and $\alpha_{\rm ex}$ is the polarizability of the obstacle along the x direction. The term $A_{\rm x}$ is the lattice structure correction term given by

$$A_{x} = \frac{1}{4\pi} \sum_{k} \frac{1}{r_{k}^{3}} \left[1 - 3 \left(\frac{x_{k}}{r_{k}} \right)^{2} \right]$$

where \vec{r}_k is the vector from the center of the "Lorentz Sphere" to the kth obstacle and \mathbf{x}_k is the x component of this vector, the summation being carried out over the sphere. Similar expressions hold for the other components. Physically speaking, the correction terms represent the polarizing effect of the other obstacles in the Lorentz sphere.

Corkum⁸ has attempted to check the Clausius-Mossotti equations experimentally for spherical obstacles. He used the Short circuit-Open circuit method at 6 cms. in rectangular guide. The obstacles were placed in a cubic array and were supported in polystyrene foam. He observed large deviations in the measured values of k_e and k_m as the sample length was changed and hence could not check equation (2:3:1). Despite these discrepancies the measured values of the refractive index were consistent. This unusual behaviour was also noted in the measurements made with the disc arrays in this work and it will be discussed in a later section. Corkum found that the experimental value of n agreed favourably with the value given by equation (2:3:2).

Lewin has derived a method of finding the relative permeability and dielectric constant of a cubic array of spheres of dimensions much smaller than a wavelength. He made use of electromagnetic scattering relations derived by Mie. The final expressions are, however, the same as the Clausius-Mossotti equations. Nevertheless, by considering the effect of the

finite conductivity of the spheres, he was able to obtain expressions for the loss tangents. Susskind has suggested that the disc array might be treated in a similar fashion, although he admits the mathematical difficulties would be great.

An electrolytic tank method has been devised by S.B.Cohn¹⁵ for the measurement of the static dielectric constant of any array of obstacles. The principle of the method is based on the well-known analogy between displacement flux lines in space and current flow lines in an electrolyte. Since the medium can be reduced by symmetry considerations to a single rectangular cell containing one obstacle, a measurement of the relative conductance of an electrolytic cell model gives an estimate of the dielectric constant. Susskind⁹ summarizes his experimental measurements of circular and square discs and compares them with values calculated by the Clausius-Mossotti relation. Large deviations between calculated and experimental values occur for closely packed arrays ie: - for large N's.

Recently, an entirely new and perhaps completely rigorous analysis of the propagation characteristics of artificial dielectrics has been developed independently by several authors ¹⁶. It is based on an electromagnetic extension of the cellular method of solid state physics. The calculations involved in the numerical evaluation of the propagation constants in such media by this method are extremely difficult and as yet no reliable results have been published. It is probably true, however, that any rigorous analysis would suffer from a similar disadvantage.

C. Flammer has been the first to publish a paper concerned with a three dimensional structure which considers many obstacle shapes, and the principles of his procedure will be outlined briefly here.

From the symmetry of the lattice, the problem of the solution of the

2:3 - 18 -

wave equation for a field component is reduced to finding the Block wave function

$$\Phi(\vec{r}) = u(\vec{r}) \exp(j \vec{K} \cdot \vec{r})$$

in a unit cell defined by the planes perpendicular to the lines joining each lattice point to its nearest neighbours. The wave function must be continuous with continuous normal derivative at the boundary of each cell. The problem then is to find a solution of Maxwell's Equations which satisfies the well-known boundary conditions at the surface of the obstacle in the cell and is such that the field components satisfy the conditions mentioned above at the boundary on the unit cell. This problem has been put into variational form by Flammer and the wave number vector, \vec{K} , can be obtained, in principle, by using the vector wave functions appropriate to the obstacle in question as the trial functions in the Rayleigh-Ritz procedure. Because of the labour involved in such a procedure, it has not as yet been used to obtain numerical results. Flammer has obtained numerical data by a very approximate procedure of numberical evaluation of the surface integrals involved in the variational problem similar to that used by Slater 18. In this case the conditions at the boundary of the unit cell are satisfied at only four points, the mid-points of each pair of faces. These results were given only to illustrate the general features of propagation in such media and are not compared with experimental measurements. Flammer has indicated that more accurate results are forthcoming.

It was mentioned before that all the existing theories which might be applicable to disc shaped array of obstacles have not considered the effect of finite conductivity. However, Carruthers, in an attempt to explain the absence of the large diamagnetic effect in the aluminum powder artificial dielectrics, has considered the effect of the conductivity on the magnetic polarizability of a disc with a thickness of the order of skin depth. He

observed, that for infinitely conducting obstacles, the impedance presented to the emf induced by the high frequency field is purely reactive, thus resulting in a diamagnetic effect. This impedance would be somewhat resistive if the conductivity is finite. He assumed this resistive component is negligible for a disc with a thickness much greater than skin depth and showed that the impedance is mainly resistive for thicknesses less than skin depth. The aluminum particles in the dielectrics measured by Vogan⁴ had thicknesses of this order and these considerations gave a possible explanation of the diamagnetic permeabilities close to unity as well as the high magnetic losses.

Chapter 3 Experimental Measurements, Apparatus and Theory

3:1 Description of the Apparatus

All measurements were taken at a free space wavelength of 3.2 cms. in a waveguide excited in the TE10 mode by a 2K39 Reflex Klystron oscillator. The Klystron was operated by a P.R.D. Type 801 Power Supply using square wave modulation with a modulation frequency which was adjustable at around 1000 cps. In Figure 2 a schematic diagram of the experimental set-up is shown. The oscillator output was fed to the waveguide by a short coaxial line and an adjustable stub matching device was placed nearby. A 10 db attenuator was used to isolate the oscillator. The absorption type cavity wave meter placed before the attenuator was calibrated in terms of guide wavelengths. Variable flap attenuators were used to vary the power passed to the standing wave section of the guide. An adjustable stub matching section served to match into the standing wave section which was of high Q.

The standing wave detector was an accurate instrument made by P.R.D. A vernier scale which could be read to one-ten thousandth of an inch was added to the commercially built standing wave section. The power sampled was detected by a 1N23A crystal and audio signal was amplified by a high gain linear amplifier and then rectified, the resulting direct current appearing on a D.C. microammeter. The short used was the same as that which E.L. Vogan describes in his report.

All dielectric samples were measured at a frequency corresponding to a guide wavelength, λ_{go} , of 4.4705 cms. To do this, the cavity gap spacing of the Klystron had to be adjusted to counteract the effect of temperature changes in the laboratory. However, during any one measurement the Klystron output was stable and the changes in the guide wavelength were negligible.

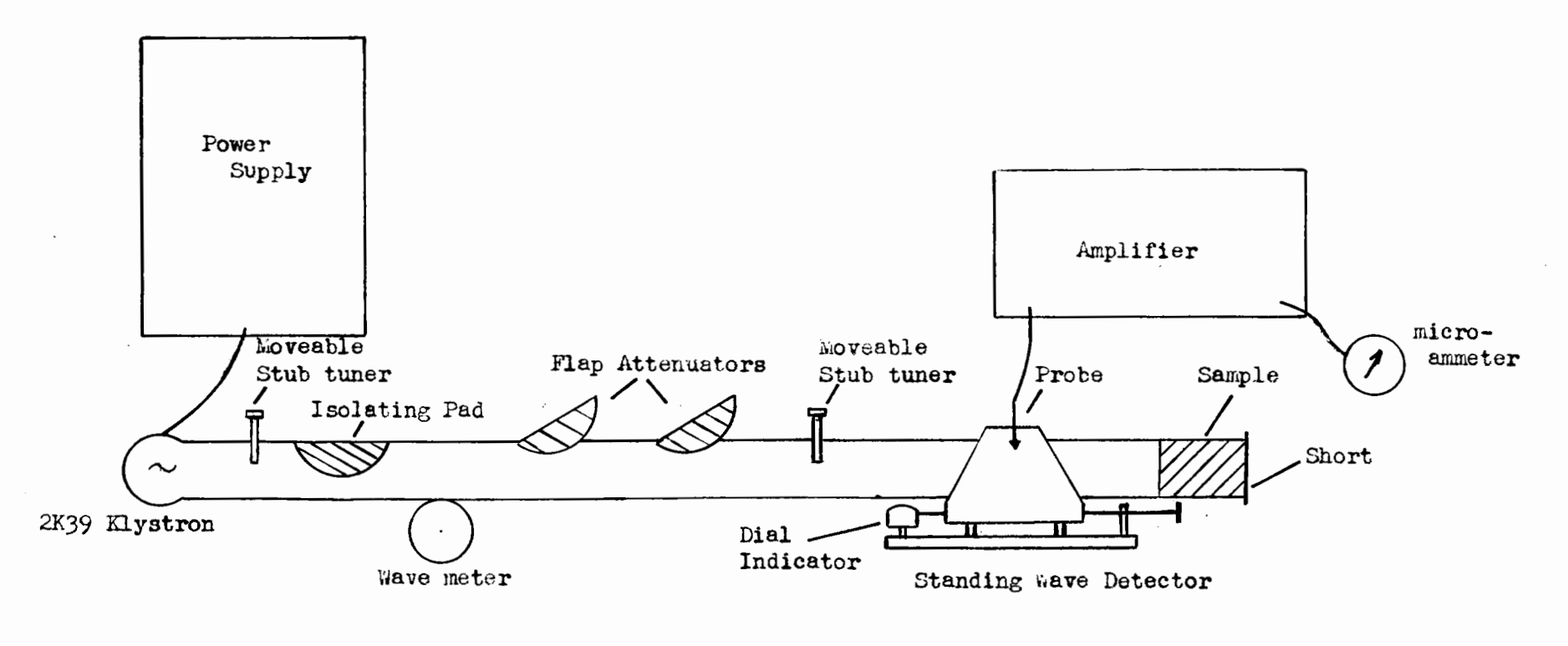


Figure 2. Schematic diagram of experimental apparatus.

The voltage standing wave ratios were obtained by the twice minimum technique rather than by the direct method. This is done by measuring the distance between the two probe positions at which the power detected is twice the power at the minimum. The inverse standing wave ratio, E_0 is then given by 5

$$E_{o} = \frac{1}{\sqrt{1 + \csc^{2} \frac{\pi \Delta X}{\lambda_{go}}}}$$

$$= \frac{\pi}{\lambda_{go}} \Delta X$$

where AX is the distance between the two twice minimum points. The approximate relation is valid to within 1 percent for inverse standing wave ratios less than 1/133. This technique has many advantages over the direct method if large standing wave ratios are measured. The effect of the nonlinearity of the crystal power response is negligible. Also, this method does not require the use of a calibrated attenuator and hence the errors associated with such an instrument are avoided. In addition, since the probe is in the region of low field at all times during the measurement, the errors associated with the probe are greatly reduced. It also might be pointed out that the position of the minimum is more accurately determined by averaging these two probe position points, rather than by finding the position of zero slope in the standing wave pattern. Using this technique, standing wave ratios as high as 500 could be measured and the losses associated with the waveguide walls could be determined, thus resulting in more accurate estimates of the losses present in the dielectric samples.

3:2 Propagation Constants and Wave Impedances in Rectangular Waveguides

It will be shown in the next section that the Short circuit - Open circuit method of measuring the magnetic and electric parameters of a dielectric can be applied to certain homogeneous anisotropic media if the corresponding propagation constants and characteristic wave impedences can be found. These quantities will be derived in this section by making use of Generalized Telegraphist's Equations obtained by Schelkunoff¹⁹ in a recent paper. The analysis involved in setting up and solving these equations for the anisotropic media of particular interest in this thesis is extremely lengthy. For this reason, and also since Schelkunoff considered a gyromagnetic medium as an example to illustrate the principles involved in the analysis, complete derivations will not be given. However, an attempt will be made to make the final results seem more plausible by first considering the simple telegraphist equations associated with the modes of propagation in a rectangular guide filled with a homogeneous isotropic dielectric.

The ordinary telegraphist equations of transmission line theory are

$$\frac{dV}{dz} = -ZI$$

$$\frac{dI}{dz} = -YV$$

where I and V are the current and voltage respectively at a point z of the line and Y and Z are the distributed shunt admittance and series impedance respectively. Equations which are formally similar to these can be obtained for each of the modes of the propagation in a guide. For the TEpq mode (the square bracket will henceforth refer to TE modes) in rectangular guide the equations are 20

$$\frac{dV}{dz}[pq] = -Z[pq]I[pq] \qquad ...(3:2:1)$$

$$\frac{d\mathbf{I}}{d\mathbf{z}}[\mathbf{p}\mathbf{q}] = \mathbf{Y}[\mathbf{p}\mathbf{q}] \mathbf{V}[\mathbf{p}\mathbf{q}] \qquad \dots (3:2:2)$$

where Y [pq] and Z [pq] are to be defined later. The quantities I [pq] and V [pq] which are functions of z only, have dimensions of current and voltage respectively, but cannot be interpreted as such in any simple manner. They are obtained from vector and scalar potentials which may be used to describe transverse electric plane waves. The scalar potential, U, can be introduced since there is no longitudinal electric current, the transverse magnetic intensity being the negative of its gradient. Also, since

$$\nabla \cdot \vec{E} = \frac{\partial E_x}{\partial x} + \frac{\partial E_y}{\partial y} = 0$$

the transverse electric intensity can be represented by the curl of a vector $\vec{\mathbf{F}}$ which has only a z-component, \mathbf{Y} , usually called a stream function. In this case the curl operator operating on $\vec{\mathbf{F}}$ reduces to

$$\nabla \times \vec{F} = \frac{2}{2} \vec{y} \vec{i} - \frac{2}{2} \vec{y} \vec{j}$$

and is usually denoted by flux y. Both the scalar potential and stream function will depend on (x,y,z), the position coordinate in the guide. However, each can be represented by the product of a function of z, and a function of x and y where the latter is a solution of the partial differential equation

$$\frac{\partial^{2}T(xy)}{\partial x^{2}} + \frac{\partial^{2}T(xy)}{\partial y^{2}} = - \chi^{2}T(xy) \qquad ...(3:2:3)$$

subject to the boundary conditions

$$\frac{\partial \underline{T}(oy)}{\partial \underline{T}(oy)} = \frac{\partial \underline{T}(ay)}{\partial \underline{X}} = \frac{\partial \underline{T}(xo)}{\partial \underline{Y}} = \frac{\partial \underline{T}(xb)}{\partial \underline{Y}} = 0$$

where a and b are the x and y dimensions of the guide respectively. If the eigenvalues and eigenfunctions are represented by χ_{pq} and $T_{pq}(xy)$, V_{pq} and V_{pq} can be written

$$U_{[pq]} = f_{[pq]}(z) \cdot T_{[pq]}(xy)$$
 ...(3:2:4)

$$y_{[pq]} = f_{2[pq]}(z) \cdot T_{[pq]}(xy).$$
 ...(3:2:5)

It might be expected that $f_{\lfloor pq\rfloor}(z)$ could be interpreted as a voltage which depends on the position along the waveguide. Also, $f_{2\lfloor pq\rfloor}(z)$ can be interpreted as a current similar to the current at a point on a transmission line. Hence, writing

$$f_{2[pq]}(z) = -I_{[pq]}(z)$$

equations (3:2:4) and (3:2:5) become

$$\gamma_{pq} = -I_{pq} \cdot T_{pq}$$
.

It is not difficult to show by Maxwell's equations that I_{pq} and V_{pq} defined in this way satisfy the telegraphist equations, (3:2:1) and (3:2:2)

if
$$Y_{[pq]} = j\omega_{\epsilon} + \frac{\chi^{2}_{[pq]}}{j\omega_{\mu}}$$
 ...(3:2:6)

and
$$Z_{[pq]} = j\omega \omega$$
. ...(3:2:7)

A solution of the form

$$V_{[pq]} = \hat{V}_{[pq]} \exp \left(Y_{i[pq]} z \right)$$

$$I_{[pq]} = \hat{I}_{[pq]} \exp \left(Y_{i[pq]} z \right)$$

where $\hat{I}_{[pq]}$ and $\hat{V}_{[r1]}$ are constant amplitude factors, is obtained if

$$Y_{i[pq]} = j\frac{\omega}{c} \left(\frac{\mu \epsilon}{\mu_o \epsilon_o} - \frac{\chi_{[pq]}^2 \chi^2}{4\pi^2} \right)^{1/2}$$

(3:2) - 26 -

For a T^{\pm} [10] mode the expression for the propagation constant becomes

$$Y_{i[10]} = Y_{i} = j\frac{\omega}{c} \left(\frac{\mu \epsilon}{\mu_{o} \epsilon_{o}} - \frac{\lambda^{2}}{\lambda_{c}^{2}}\right)^{1/2}$$

since
$$\chi^2_{[10]} = \frac{4\pi^2}{\lambda_c^2}$$
.

The characteristic wave impedance Z_{ki} [pq] can also be obtained from the telegraphist equations by the well-known relation

$$Z_{ki[pq]} = \sqrt{\frac{Z_{pq}}{Y_{pq}}} = \frac{j\omega L}{V_{i[pq]}}$$

If scalar and stream functions V' and II are introduced to describe the transverse electric and magnetic intensity of TM modes, equations of the form (round brackets surrounding subscripts will henceforth refer to TM modes)

$$\frac{\mathrm{d}\mathbf{v}(\mathbf{p}\mathbf{q})}{\mathrm{d}\mathbf{z}} = -\left(\mathbf{j}\omega\boldsymbol{\epsilon} + \frac{\boldsymbol{\chi}_{(\mathbf{p}\mathbf{q})}^{2}}{\mathbf{j}\omega\boldsymbol{\mu}}\right) \mathbf{I}_{(\mathbf{p}\mathbf{q})} \qquad \dots (3:2:8)$$

$$\frac{dI}{dz}(pq) = - j\omega \epsilon V(pq) \qquad ...(3:2:9)$$

are obtained where $V_{(pq)}$ and $I_{(pq)}$ are related to the potential and stream functions in the following way:

$$V'_{(pq)} = - V_{(pq)}(z) T_{(pq)}(xy)$$

$$\Pi_{(pq)} = - I_{(pq)}(z) T_{(pq)}(xy)$$
.

 $T_{(pq)}$ is a solution of equation (3:2:3) subject to the boundary conditions.

$$T(oy) = T(ay) = T(xo) = T(xb) = 0$$

Also, by solving this problem, the eigenvalues $X_{(p \cap)}$ are obtained. Then, the propagation constant and characteristic impedance can be derived in a manner similar to that outlined previously in the transverse electric case.

To summarize, the system of equations

$$\frac{d\mathbf{v}}{d\mathbf{z}}[\mathbf{p}\mathbf{q}] = -\mathbf{z}[\mathbf{p}\mathbf{q}] \quad \mathbf{I}[\mathbf{p}\mathbf{q}] \qquad \dots (3:2:10a)$$

$$\frac{dI}{dz}[pq] = -Y_{[pq]} V_{[pq]} \qquad ...(3:2:10b)$$

$$\frac{dV}{dz}(pq) = -Z(pq) I(pq) \qquad ...(3:2:10c)$$

$$\frac{dI}{dz} pq) = -Y_{(pq)} V_{(pq)} \qquad ...(3:2:10d)$$

along with the T functions can be used to describe completely wave propagation in a homogeneous, isotropic, dielectric filled, rectangular guide.

The problem of wave propagation in an anisotropic medium bounded by perfectly conducting guide valls would be extremely difficult if attacked in the conventional way, that is, as a boundary value problem. The approach used by Schelkunoff, although quite mathematical, was motivated by the following physical reasoning. From equations (3:2:10) the electromagnetic boundary value problem for a homogeneous isotropic medium can be transformed into the problem of the solution of an infinite set of independent ordinary differential equations resembling the familiar telegraphist's equations.

Each equation corresponds to one of the modes of propagation in the guide. If any irregularity is introduced into the guide, coupling may arise between some or all of these modes and the solution of this new problem is obtained by a judicious combination of the uncoupled normal mode solutions. This ensures that the boundary conditions at the waveguide walls are satisfied. The irregularity may take the form of discontinuity in the guide or an enisotropy in the dielectric. In terms of the transmission line analogy,

this coupling may be represented by distributed transfer impedances and admittances (or transfer coefficients). Hence, the Generalized Telegraphist's Equations take the following form if tensor notation is used.

$$\frac{dV}{dz}(pq) = - Z_{(pq)(st)} I_{(st)} - Z_{(pq)(st)} I_{(st)} - Z_{(pq)(st)} I_{(st)} - V_{(pq)(st)} V_{(st)} - V_{(pq)(st)} V_{(st)} - V_{(pq)(st)} V_{(st)} - V_{(pq)(st)} V_{(st)} - V_{(pq)(st)} I_{(st)} - V_{(pq)(st)} I_{(st)} - I_{(pq)(st)} I_{(st)} - V_{(pq)(st)} I_{(st)} - I_{(pq)(st)} I_{(st)} - I_{(pq)(st$$

...(3:2:11d)

where p,q,s,t, take on positive integral values. By making use of relations between the I's, V's and T's and the electromagnetic field components, and with the help of the Maxwell's Equations, Schelkunoff obtained expressions for the transfer coefficients in the form of integrals involving permeability and permittivity tensor components and derivatives of the T(xy) functions. For the general anisotropic medium these coefficients are extremely complicated. Schelkunoff treats the case of a medium isotropic in its dielectric properties, but with ferromagnetic properties characterized by the tensor

(3:2) - 29 -

$$(\mu) = \begin{pmatrix} \mu & \mu_{1} & 0 \\ \mu_{1} & \mu & 0 \\ 0 & 0 & \mu_{2} \end{pmatrix}$$

He shows how the propagation constant for the TE [lo] mode is modified due to coupling with the TE [lo] mode. Also, if the mutual permeability, μ_1 , is zero, he shows that there is no coupling, the only modification being a change in [lo] which is

$$\gamma_{\text{[jo]}} = j_{c}^{\underline{\omega}} \left(\frac{\mu \epsilon}{\mu_{o} \epsilon_{o}} - \frac{\mu \lambda^{2}}{\mu_{2} \lambda_{c}^{2}} \right)^{1/2}.$$

One of the anisotropic media of particular interest here is that characterized by the tensors

$$(\epsilon) = \begin{pmatrix} \epsilon_0 & 0 & 0 \\ 0 & \epsilon & 0 \\ 0 & 0 & \epsilon \end{pmatrix} \quad \text{and } (\mu) = \begin{pmatrix} \mu & 0 & 0 \\ 0 & \mu_0 & 0 \\ 0 & 0 & \mu_0 \end{pmatrix}$$

where ϵ_0 and μ_0 are the permittivity and permeability of free space, respectively. Such is the case for a disc array medium in which the disc faces lie parallel to the yz plane (see Figure 1a). The z axis coincides with the propagation direction of the waveguide. The derivation of the transfer coefficients for this medium follows closely with that of the special case treated by Schelkunoff, hence it will not be given here. It might be mentioned, however, that the integrals involved are somewhat different. The coefficients $\mathrm{VT}_{(pq)(st)}$, $\mathrm{IT}_{[pq](st)}$ are all zero and the transfer impedances and admittances are given by the following relations:

$$Z_{(pq)(st)} = \frac{j\omega\pi^2}{X_{(pq)}X_{(st)}} \left(\frac{tq\mu}{a^2} + \frac{ps\mu_0}{b^2}\right) + \frac{X_{(pq)}^2}{j\omega\epsilon} \quad \text{if } p = s$$

= 0 for all other cases.

(3:2)- 30 -

$$Z_{(pq)}[st] = \frac{j\omega \pi^2}{\chi_{(pq)}\chi_{[st]}ab} (sq\mu - pt\mu_0)$$
 if $p = s$

= 0 for all other cases.

$$Y_{(pq)(st)} = \frac{j\omega\pi^2}{X_{(pq)}X_{(st)}} \left(\frac{sp\epsilon_0}{a^2} + \frac{tq\epsilon}{b^2}\right)$$
 if $t = q$

= 0 for all other cases.

$$Y_{(pq)[st]} = \frac{j\omega\pi^2}{X_{(pq)}X_{[st]}ab} (sqe - pte_0) \quad if \quad p = s$$

= 0 for all other cases.

$$Z_{\text{[pc][st]}} = \frac{j\omega\pi^2}{\chi_{\text{(pq)}}\chi_{\text{[st]}}} \left(\frac{\text{sp}\mu}{\text{a}^2} + \frac{\text{tq}\mu_0}{\text{b}^2}\right) \quad \text{if} \quad p = s$$

= 0 for all other cases.

$$Z_{pq}(st) = \frac{j\omega\pi^2}{\chi_{pq}\chi_{st}^{ab}} (tp\mu - sq\mu_0)$$
 if $p = s$

= 0 for all other cases.

Y[pq][st] =
$$\frac{j\omega\pi^2}{\mathbf{X}[pq]\mathbf{X}[st]}$$
 $\left(\frac{sp\epsilon}{a^2} + \frac{tq\epsilon_0}{b^2}\right)$ + $\frac{\mathbf{\chi}[pq]}{j\omega\mu_0}$ if $p = s$ = 0 for all other cases.

$$Y_{\text{[pq](st)}} = \frac{j\omega\pi^2}{\chi_{\text{[pq]}}\chi_{\text{(st)}}^{\text{ab}}} \quad (\text{tr} \epsilon - \text{sq} \epsilon_0) \qquad \text{if} \quad p = s \\ t = q$$

= 0 for all other cases.

and

If the TE [10] mode is propagated in a guide filled with this anisotropic medium, the only non-zero coefficients appearing in the last two

telegraphist equations are
$$Y_{[10][10]} = Y_{[10]} = j\omega \epsilon + \frac{\chi_{[10]}^2}{j\omega\mu_0}$$
 and
$$Z_{[10][10]} = Z_{[10]} = j\omega\mu.$$

by comparison with equations (3:2:6) and (3:2:7) it is seen that only the second term in $Y_{[10]}$ is changed, the μ being replaced by μ_{0} .

(3:2) - 31 -

Since there is no coupling with the transverse magnetic modes the last two telegraphist equations

$$\frac{dV}{dz}[10] = -j\omega t I_{[10]}$$

$$\frac{dI}{dz}[10] = -(j\omega \epsilon + \frac{2^2 L0}{j\omega t}) V_{[10]}$$

are independent of the first two and can be solved by assuming a solution of the form

$$v_{[10]} = \hat{v}_{[10]} \exp(Y_{i[10]}z),$$

$$v_{[10]} = \hat{v}_{[10]} \exp(Y_{i[10]}z).$$

This solution gives

$$Y_{\text{i[lo]}} = j\frac{\omega}{c} \left(\frac{\mu \epsilon}{\mu_{\text{o}} \epsilon_{\text{o}}} - \frac{\mu}{\mu_{\text{o}}} \frac{\lambda^{2}}{\lambda_{\text{c}}^{2}} \right)^{1/2}$$
 since $X_{\text{[lo]}}^{2} = \frac{\mu r^{2}}{\lambda_{\text{c}}^{2}}$. The characteristic wave impedance $Z_{\text{ki[lo]}}$ defined by
$$Z_{\text{ki[lo]}} = \sqrt{\frac{Z_{\text{[lo]}}}{Y_{\text{[lo]}}}}, \text{ then becomes}$$

 $z_{ki[10]} = \frac{j\omega\mu}{\gamma_{i[10]}}$

It will be seen in Chapter 5 that in order to determine accurate values of the electric and magnetic parameters for the disc array it was necessary to take measurements for two different orientations of sample in the guide. One of these is the one considered above. The other is that for which the planes of the discs coincide with the xy plane. By referring to Figure 1b, it is easily seen that in the latter case the tensors (\mathcal{E}) and (μ) become

(3:2)
$$-32 -$$

$$(\epsilon) = \begin{pmatrix} \epsilon & 0 & 0 \\ 0 & \epsilon & 0 \\ 0 & 0 & \epsilon \end{pmatrix} \text{ and } (\mu) = \begin{pmatrix} \mu_0 & 0 & 0 \\ 0 & \mu_0 & 0 \\ 0 & 0 & \mu \end{pmatrix}$$

Again, for this case the transfer coefficients ${}^{V}T$'s and ${}^{I}T$'s are zero and the only non-zero transfer impedances and admittances are

$$Z_{(pq)(st)} = + (j\omega t_0 + \frac{\chi^2_{(pq)}}{j\omega \epsilon})$$
 if $s = p$
= 0 for all other cases.

$$Y_{(pq)(st)}$$
 = + $j\omega \in \text{if } s = p$
 $q = t$
 = 0 for all other cases.

Y [pq][st] = + (j
$$\omega \epsilon$$
 + $\frac{\chi^2_{pq}}{j\omega \mu}$) if $s = p$
= 0 for all other cases.

Thus, as before, the last two telegraphist equations do not contain any coefficients which couple them with the corresponding equations for the transverse magnetic modes. The equations for a TE_[10] mode become

$$\frac{dV}{dz}[10] = -j\omega\mu_0 I[10]$$

$$\frac{dI}{dz}[10] = -(j\omega\epsilon + \frac{\chi^2_{10}I}{j\omega\mu}) V_{[10]}.$$

Again, assuming a solution of the form

$$I_{[lo]} = \hat{I}_{[lo]} \exp(\hat{Y}_{i[lo]}z)$$

$$V_{\text{Ilo]}} = \hat{V}_{\text{Ilo]}} \exp(Y_{\text{illo]}z})$$

the expression for the propagation constant becomes

$$\gamma_{i[10]} = j\frac{\omega}{c} \left(\frac{\epsilon}{\epsilon_0} - \frac{\mu_0}{\mu} \frac{\lambda^2}{\lambda_c^2} \right)^{1/2}$$

The characteristic wave impedance obtained by taking the square root of the ratio $Z_{\Pi \Pi}/Y_{\Pi \Pi}$ becomes in this case

$$Z_{ki[lo]} = \frac{j\omega \mu_0}{\gamma_{i[lo]}}$$
.

In order to distinguish the propagation constants and characteristic impedance for this orientation from that of the previous, the subscript 2 will be substituted for the subscript [10]. The subscript 1 will be used when referring to the previous orientation treated.

3:3 Theory of the Short circuit - Open circuit Weasurements

The measurement is based on the fact that the input impedance, Z_b , near the generator end of a section of a dielectric filled waveguide can be expressed in terms of the distance from the dielectric to the first voltage minimum, X, and the inverse standing wave ratio, E, both of which can be measured. This input impedance can also be expressed in terms of the termination impedance at the opposite end of the dielectric sample, the propagation constant in the medium and the thickness of the sample by a well-known transmission line relation. If the termination impedance is a short circuit, the expression is relatively simple and the propagation constant in the dielectric filled guide is simply related to E, and X. If the expression for Y_i is known, the properties of the medium may be expressed in terms of E, and X. If the medium is a pure dielectric ($\mu = \mu_0$ and $\tan \delta_m = 0$) k_0 and $\tan \delta_0$

are then expressible in terms of E, and X. If, however, the medium has magnetic properties, the short circuit termination measurements are not sufficient. To obtain another independent relation, E, and X must be measured for a different termination impedance. A termination which yields a relatively simple relation and which at the same time is easily realized in practice is the open circuit impedance obtained by displacing the sample one-quarter of a wavelength from a perfect short. In the following analysis explicit relations are established between the parameters of the medium and the quantities measured.

The transmission line relation which is basic in the whole of the theory is that which expresses $\mathbf{Z}(\mathbf{z})$, the impedance at a distance \mathbf{z} from a waveguide termination of impedance \mathbf{Z}_t in terms of \mathbf{z} , \mathbf{Z}_t and $\mathbf{Y} = \mathbf{\alpha} + \mathbf{j}\mathbf{\beta}$, the propagation constant in the guide, namely

$$\frac{Z(z)}{Z_k} = \frac{Z_t + Z_t \tanh Yz}{Z_k + Z_t \tanh Yz} \qquad \dots (3:3:1)$$

where \mathbf{Z}_k is the characteristic impedance. For the lossless case $\boldsymbol{\gamma}$ is equal to $j\beta$ and equation (3:3:1) becomes

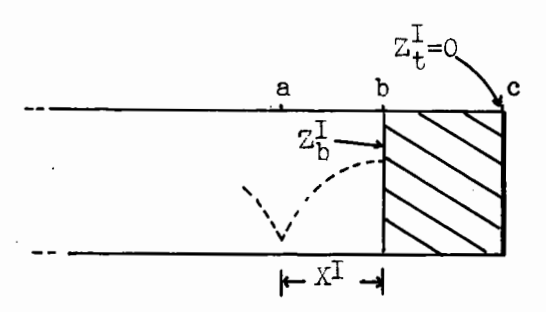
$$\frac{Z(z)}{Z_k} = \frac{Z_t + jZ_k \tan \beta z}{Z_k + jZ_t \tan \beta z}$$
 ...(3:3:2)

These equations can be obtained by solving the ordinary telegraphist equations

$$\frac{dV}{dz} = ZI, \quad \frac{dI}{dz} = YV$$

subject to certain conditions at the termination. In order to emphasize the similarity of the short circuit and open circuit theory, the analogous relations in each will appear side by side in the following two columns. The superscripts I and II refer to the short and open terminations

respectively and Z_b is the impedance at the front face of the dielectric. Also, Z_{ko} represents the characteristic wave impedance in an empty guide and Z_{ki} the characteristic wave impedance in a dielectric filled guide.



By applying relation (3:3:2) to section ab of the guide, the expression for the normalized impedance at the first minimum becomes

$$z(x^{I}) = \frac{z(x^{I})}{z_{ko}} = \frac{z_{b}^{I} + jz_{ko} \tan \beta_{o} x^{I}}{z_{ko} + jz_{b}^{I} \tan \beta_{o} x^{I}}$$

$$\cdots (3:3:3)^{I}$$

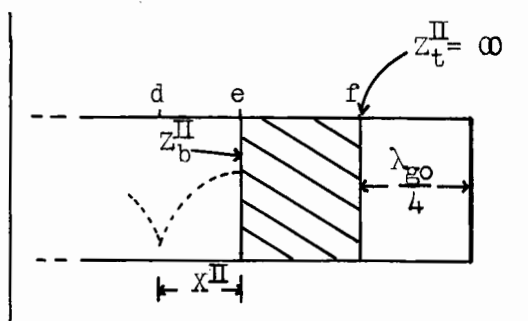
It is easily shown that $z(x^{I})$ is related to \mathbf{E}_{o}^{I} in the following way⁵

$$z(X^{I}) = E_{o}^{I}$$

and hence by (3:3:3)I

$$\mathbf{z}_b^{\mathbf{I}} = \frac{\mathbf{z}_b^{\mathbf{I}}}{\mathbf{z}_{ko}} = \frac{\mathbf{z}_o^{\mathbf{I}} - \mathbf{j} \mathrm{tan} \boldsymbol{\beta}_o \mathbf{X}^{\mathbf{I}}}{\mathbf{1} - \mathbf{j} \mathbf{E}^{\mathbf{I}} \mathrm{tan} \boldsymbol{\beta} \mathbf{X}^{\mathbf{I}}}$$

= S^{I} exp(jT^{I}) ...(3:3:4)^I where S^{I} and T^{I} can be obtained from E_{0}^{I} and X^{I} .



By applying relation (3:3:2) to section de of the guide, the expression for the normalized impedance at the first minimum

becomes
$$z(x^{\text{II}}) = \frac{z(x^{\text{II}})}{z_{\text{ko}}} = \frac{z_{\text{b}}^{\text{II}} + jz_{\text{ko}} \tan \beta_{\text{o}} x^{\text{II}}}{z_{\text{ko}} + jz_{\text{b}} \tan \beta_{\text{o}} x^{\text{II}}}$$

$$\cdots (3:3:3)^{\text{II}}$$

It is easily shown that $z(x^{11})$ is related to E_0^{11} in the following way⁵

$$z(X^{\Pi}) = E_0^{\Pi}$$

and hence by $(3:3:3)^{II}$

$$z_b^{II} = \frac{z_b^{II}}{z_{ko}} = \frac{z_o^{II} - j \tan \beta_o X^{II}}{1 - j E^{II} \tan \beta_o X^{II}}$$

= S^{II} exp(jT^{II}) ...(3:3:4) where S^{II} and T^{II} can be obtained from E_0^{II} and X^{II} .

(3:3)- 36 -

By applying (3:3:1) to the section bc the normalized impedance at the face of the dielectric becomes

$$z_b^{I} = \frac{z_b^{I}}{z_{ki}} = \tanh Y_i d$$

$$\dots (3:3:5)^{I}$$

By a comparison of $(3:3:4)^{I}$ and (3:3:5) a relationship between the measured quantity S^Iexp(jT^I) and quantities characteristic of the medium and the guide is obtained which is

$$S^{I} \exp(jT^{I}) = \frac{Z_{ki}}{Z_{ko}} \tanh \Upsilon_{id}$$

$$\dots(3:3:6)^{I}$$

$$S^{II} \exp(jT^{II}) = \frac{Z_{ki}}{Z_{ko}} \frac{1}{\tanh \Upsilon_{id}}$$

By applying (3:3:1) to the section ef the normalized impedance at the face of the dielectric becomes

$$z_b^{II} = \frac{z_b^{II}}{z_{ki}} = \frac{1}{\tanh \gamma_i d} \cdots (3:3:5)^{II}$$

By comparison of $(3:3:4)^{II}$ and (3:3:5) a relationship between the measured quantity S exp(jT) and quantities characteristic of the medium and the guide is obtained which is

$$S^{II} \exp(jT^{II}) = \frac{Z_{ki}}{Z_{ko}} \frac{1}{\tanh \gamma_{id}} \dots (3:3:6)^{II}$$

By suitable manipulations of equations $(3:3:6)^{I}$ and $(3:3:6)^{I}$ the following two important relations can be obtained:

$$\frac{Z_{ki}}{Z_{ko}} = \sqrt{S^{I} S^{II}} \exp(j \frac{T^{I} + T^{II}}{2}) = B \exp(j\emptyset) \qquad ...(3:3:7)$$

$$\frac{\Upsilon_{i}}{\Upsilon_{o}} = \frac{\lambda_{go}}{j2\pi d} \tanh^{-1} \left[\sqrt{\frac{S^{I}}{S^{II}}} \exp \left(j\frac{T^{I} - T^{II}}{2}\right) \right] = A \exp(-j\theta) \dots (3:3:8)$$

where A, B, Θ and \emptyset are introduced for convenience in the discussions which follow and of is the propagation constant in an empty waveguide and is given by

$$\gamma_{\rm o} = j\frac{\omega}{c} (1 - \lambda^2 \wedge_{\rm c}^2)^{1/2} = j2\pi \wedge_{\rm go}$$

(3:3) - 37 -

Homogeneous, Isotropic Dielectric:-

If the medium is homogeneous and isotropic in both its electric and magnetic properties then

$$\gamma_i = j \frac{\omega}{c} \left(\frac{\mu \epsilon}{\mu_0 \epsilon_0} - \frac{\lambda^2}{\lambda_c^2} \right)^{1/2}$$

and

$$z_{ki} = \frac{j\omega \iota}{\gamma_i}$$
.

The characteristic wave impedance in an empty guide, Z_{ko} , is $j\omega L_o/\gamma_o$ and hence equations (3:3:7) and (3:3:8) become

$$\frac{\mu V_0}{\mu_0 r_i} = B \exp(j\emptyset) \qquad \dots (3:3:9)$$

and

$$\frac{Y_{i}}{Y_{0}} = A \exp(-j\theta). \qquad ...(3:3:10)$$

From the definition of $tand_m$, the ratio $\frac{\mu}{\mu_0}$ becomes $k_m(1 - jtand_m)$ and if (3:3:9) is multiplied by (3:3:10) the relation

$$k_{\rm m}(1 - j tan \delta_{\rm m}) = AB \exp j(\emptyset - \Theta)$$

is evident. Upon equating moduli and angles the following relations for ${\tt tanb}_m$ and ${\tt k}_m$ result:

$$tanb_{m} = -tan(\emptyset-\Theta) \qquad ...(3:3:11)$$

$$k_{\rm m} = \frac{AB}{1 + \tan^2 \delta_{\rm m}}$$
 ...(3:3:12)

It is interesting to note that these formulae are exact and hence the permeabilities and magnetic loss tangents of materials of high magnetic loss can be measured by this technique.

Provided it can be assumed that both the electric and magnetic

loss tangents of the medium are small, $k_e^{}k_m^{}$ and the total loss \geq tancan be expressed in terms of A and erespectively, in the manner outlined below:

$$\frac{\gamma_{i}}{\gamma_{o}} = \frac{j\frac{\omega}{c} \left(\frac{\mu \epsilon}{\mu_{o} \epsilon_{o}} - \frac{\lambda^{2}}{\lambda_{c}^{2}}\right)^{1/2}}{j\frac{\omega}{c} \left(1 - \frac{\lambda^{2}}{\lambda_{c}^{2}}\right)^{1/2}} = A \exp(-j\theta) \qquad ...(3:3:13)$$

and if ϵ and μ are put equal to $k_e \epsilon_0 (1 - j tan \delta_e)$ and $k_m \mu_0 (1 - j tan \delta_m)$ respectively, equation (3:3:13) becomes

$$\frac{\lambda_{go}}{\lambda} \left(k_e k_m (1 - j tanb_e) (1 - j tanb_m) - \frac{\lambda^2}{\lambda_c^2} \right)^{1/2} = A \exp(-j\theta) \qquad \dots (3:3:14)$$

Upon squaring, equation (3:3:14) becomes

$$\frac{\lambda_{go}^2}{\lambda^2} \left(k_e k_m (1 - j tanb_e) (1 - j tanb_m) - \frac{\lambda^2}{\lambda_c^2} \right) = A^2 \exp(-j2\theta)$$

or

$$\frac{\lambda_{go}^{2}}{\lambda^{2}} \left(k_{e} k_{m} \sqrt{1 + \tan^{2} \delta_{m}} \exp \left[-j \tan^{-1} (\sum \tan \delta) \right] \right) - \frac{\lambda_{go}^{2}}{\lambda_{c}^{2}}$$

$$= A^{2} \exp(-j 2e). \qquad ...(3:3:15)$$

If the loss tangents are such that the approximations

$$\sqrt{(1+\tan^2 b_e)(1+\tan^2 b_m)} \neq 1$$

$$\exp[-j\tan^{-1}(2\tan b)] \neq 1 - j2\tan b$$

are valid, then equation (3:3:15) becomes

$$\frac{\lambda_{go}^2}{\lambda^2} \left(k_e k_m - \frac{\lambda^2}{\lambda_c^2} \right) - j \frac{\lambda_{go}^2}{\lambda^2} k_e k_m (\Sigma tanb) \stackrel{:}{=} A^2 \exp(-j2\theta)$$

or

$$\frac{\lambda_{go}^{2}}{\lambda^{2}} \left(k_{e} k_{m} - \frac{\lambda^{2}}{\lambda_{c}^{2}} \right) \exp -j \frac{\lambda \tan \delta}{1 - \frac{\lambda^{2}}{\lambda_{c}^{2}} k_{e} k_{m}} \stackrel{?}{=} A^{2} \exp(-j2\theta)$$

and therefore

$$\mathbf{k}_{\mathbf{e}}\mathbf{k}_{\mathbf{m}} \doteq (\mathbf{A}^2 + \frac{\lambda_{\mathbf{go}}^2}{\lambda_{\mathbf{go}}^2})\frac{\lambda_{\mathbf{go}}^2}{\lambda_{\mathbf{go}}^2} \qquad \qquad \cdots (3:3:16)$$

and

$$\Sigma \tanh = 2(1 - \frac{\lambda^2}{\lambda_c^2 k_e k_m}) \theta$$
 ...(3:3:17)

Although (3:3:16) and (3:3:17) apply only to materials of small loss tangents, $k_{\rm e}k_{\rm m}$ and Ztanb can be obtained for materials of large loss tangents by using the approximate values given by these equations as the initial values in a method of successive approximations which may be applied to the rigorous equation (3:3:15). However, this was not necessary in any of the measurements reported in this thesis. $k_{\rm e}$ and $tenb_{\rm e}$ are easily obtained from equations (3:3:11), (3:3:12), (3:3:16) and (3:3:17). This method of deriving the relations between the parameters and the measured quartities emphasizes the fact that the values of the refractive index and the total loss tangent depend only on the values

If done in a rigorous manner, the inversion of tanh Y_id given in equation (3:3:8) is the most time consuming part of the numerical evaluation of the quantities A, B, θ and \emptyset from the measured X's and E's. In appendix A, this inversion is carried out using valid approximations resulting in a considerable reduction in the time spent on calculations. The use of this approximate procedure along with the fact that the frequency was kept the same for all measurements reduced the calculation time by about 75 percent.

The formulae used to obtain S^{I} , T^{I} , S^{II} and T^{II} are not derived here since they have been treated thoroughly elsewhere 4. It might be mentioned, however, that the values of X have been corrected to include the effect of the slotted portion of the standing wave section

and the E's have been corrected for the losses present in the wells of the guide. A typical calculation which shows these correction terms as well as the revisions introduced by the above analysis is given in Appendix A.

Homogeneous, Anisotropic Dielectrics

The propagation constant and characteristic wave impedance for the anisotropic medium first considered are

$$\gamma_{i1} = j \frac{\omega}{c} \left(\frac{\mu \epsilon}{\mu_0 \epsilon_0} - \frac{\mu}{\mu_0} \frac{\lambda^2}{\lambda_c^2} \right) \qquad ...(3:3:18)$$

and
$$Z_{kil} = \frac{j\omega L}{Y_{il}}$$
 ...(3:3:19)

If these expressions are substituted into equations (3:3:7) and (3:3:8) the following relations are apparent

$$\frac{\mu \mathbf{r}_{0}}{\mu_{0} \mathbf{r}_{11}} = B_{1} \exp(j\mathbf{r}_{1}) \qquad \dots (3:3:20)$$

$$\frac{\Upsilon_{i1}}{\Upsilon_{o}} = \frac{\lambda_{go}}{\lambda} \left(\frac{\mu \epsilon}{\mu_{o} \epsilon_{o}} - \frac{\mu}{\mu_{o}} \frac{\lambda^{2}}{\lambda_{c}^{2}} \right)^{1/2} = A_{1} \exp(-j\theta_{1}) \qquad ...(3:3:21)$$

In order to account for the loss associated with the electric and magnetic polarizations the tensor components $\pmb{\epsilon}$ and $\pmb{\mu}$ may be written

= $\epsilon_{\rm o}$ k_e(l-jtanb_e) and μ = $\mu_{\rm o}$ k_m(l-jtanb_m). Then if equation (3:3:20) is multiplied by (3:3:21) the relation

$$k_m(1-jtanb_m) = A_1B_1 \exp j(\emptyset_1 - \Theta_1)$$

results and the formulae

$$tanb_{m} = -tan(\emptyset_{1} - \Theta_{1}) \qquad ...(3:3:22)$$

and

$$k_{\rm m} = \frac{A_1 B_1}{\sqrt{1 + \tan^2 b_{\rm m}}}$$
 ...(3:3:23)

are obtained. Again it is noted that the permeability and magnetic

loss tangent of materials of high magnetic loss can be measured by this method.

By comparing equation (3:3:21) with the corresponding equation of the isotropic case, it is seen that $k_e k_m$ and $\Sigma tanb$ cannot be expressed in terms of A_1 and Θ_1 respectively. However, by the following procedure, it is possible to obtain expressions for k_e and $tanb_e$.

When squared, equation (3:3:21) becomes

$$\frac{\lambda_{\text{go}}^{2}}{\lambda^{2}} \left(\frac{\mu \epsilon}{\mu_{0} \epsilon_{0}} - \frac{\mu}{\mu_{0}} \frac{\lambda^{2}}{\lambda_{c}^{2}} \right) = A_{1}^{2} \exp(-j2\theta_{1})$$
or
$$\frac{\lambda_{\text{go}}^{2}}{\lambda^{2}} \left(k_{e} k_{m} (1-j \tan \theta_{e}) (1-j \tan \theta_{m}) - k_{m} (1-j \tan \theta_{m}) \frac{\lambda^{2}}{\lambda_{c}^{2}} \right) = A_{1}^{2} \exp(-j2\theta_{1})$$
and
$$\frac{\lambda_{\text{go}}^{2}}{\lambda^{2}} \left(k_{e} k_{m} \sqrt{1+\tan^{2}\theta_{e}} \sqrt{1+\tan^{2}\theta_{m}} \exp\left[-j \tan^{-1}(\sum \tan \theta_{m})\right] \right) = A_{1}^{2} \exp(-j2\theta_{1}).$$

$$-k_{m} \frac{\lambda_{c}^{2}}{\lambda_{c}^{2}} \sqrt{1+\tan^{2}\theta_{m}} \exp\left[-j \tan^{-1}(\tan \theta_{m})\right] \right) = A_{1}^{2} \exp(-j2\theta_{1}).$$

$$\cdots (3:3:24)$$

If the loss tangents are such that

$$\sqrt{1 + \tan^2 \delta_e} \sqrt{1 + \tan^2 \delta_m} \stackrel{?}{\Rightarrow} 1$$
 $\exp\left[-j\tan^{-1}(\Sigma \tan \delta)\right] \stackrel{?}{\Rightarrow} 1 - j\Sigma \tan \delta$

and $\exp \left[-j \tan^{-1}(\tanh_m)\right] \stackrel{:}{\cdot} 1 - j \tan \delta_m$ equation (3:3:24) becomes

$$\frac{\lambda_{go}^{2}}{\lambda^{2}} k_{e}k_{m} - k_{m} \frac{\lambda_{go}^{2}}{\lambda_{c}^{2}} - j \left(\frac{\lambda_{go}^{2}}{\lambda^{2}} k_{e}k_{m} \sum tanb - k_{m} \frac{\lambda_{go}^{2}}{\lambda_{c}^{2}} tanb_{m}\right) \doteq A_{1}^{2} \exp(-j2\theta_{1})$$
or
$$\frac{\lambda_{go}^{2}}{\lambda^{2}} k_{m} \left(k_{e} - \frac{\lambda^{2}}{\lambda_{c}^{2}}\right) \exp\left[-j \frac{k_{e} tanb_{e} + (k_{e} - \lambda^{2} \Lambda_{c}^{2}) tanb_{m}}{k_{e} - \lambda^{2} \Lambda_{c}^{2}}\right] \doteq A_{1}^{2} \exp(-j2\theta_{1})$$
...(3:3:26)

(3:3)- 42 -

Hence by equating moduli ke is given by

$$k_e = \frac{\lambda^2}{\lambda_{go}^2} \frac{A_1^2}{k_m} + \frac{\lambda^2}{\lambda_c^2}$$

and if $k_e k_m \neq A_1 B_1$ this becomes

$$k_{e} = \frac{\lambda^{2}}{\lambda_{go}^{2}} = \frac{A_{1}}{B_{1}} + \frac{\lambda^{2}}{\lambda_{c}^{2}} + \dots (3:3:27)$$

By equating the angles in equation (3:3:26)

$$\frac{\tanh_{\Theta}}{\left(1 - \frac{\lambda^2}{\lambda_c^2 k_{\Theta}}\right)} + \tanh_{m} = 2\theta_1$$

or

$$tanb_{e} \doteq (1 - \frac{\lambda^{2}}{\lambda_{c}^{2}k_{e}})(2\theta_{1} - tanb_{m})$$

$$\doteq (1 - \frac{\lambda^{2}}{\lambda_{c}^{2}k_{e}})(\theta_{1} + \emptyset_{1}). \qquad ...(3:3:28)$$

Hence, by the use of equations (3:3:22), (3:3:23), (3:3:27) and (3:3:28) approximate values of the electric and magnetic parameters can be obtained from measurements made by the Short circuit-Open circuit method. Again, if the loss tangents are not small the approximate values can be used to obtain more accurate values by the method of successive approximations applied to the rigorous formulae given in (3:3:24).

In the case of the second orientation considered in the previous section, the propagation constant and characteristic impedance are

$$Y_{12} = j \frac{\omega}{c} \left(\frac{\epsilon}{\epsilon_0} - \frac{\mu_0}{\mu} \frac{\lambda^2}{\lambda_c^2} \right) \qquad ...(3:3:29)$$

and
$$Z_{ki2} = \frac{j\omega L_0}{Y_{i2}}$$
. ...(3:3:30)

If these are substituted into equations (3:3:7) and (3:3:8), the following two relations are obtained:

$$\frac{\Upsilon_{o}}{\Upsilon_{i2}} = B_2 \exp(j \phi_2) \qquad \dots (3:3:31)$$

$$\frac{Y_{12}}{Y_0} = A_2 \exp(-j\theta_2).$$
 ...(3:3:32)

It is immediately evident that the short and open circuit terminations do not give independent relations, in which case it is impossible to solve for the required parameters k_e , k_m , $tan\delta_e$ and $tan\delta_m$.

In the next chapter it will be shown that there are comparatively large errors in B and Ø due to the errors involved in the measurement of the X's and E's. This, however, is not the case for A and O, the errors in these quantities being comparatively small. Also, it is shown that the expected error in B is a minimum when the sample length is an odd multiple of one-eighth of a wavelength and it increases rapidly as the sample length is changed from this value. Again, this is not true of A. Actually, this quantity can be measured accurately for any length, with the accuracy increasing slightly as the sample length is increased. Because of these facts, it might be necessary to measure the disc array samples for the two orientations in the guide. If this is done, the four electric and magnetic parameters can be obtained from the relations

$$\frac{Y_{11}}{Y_0} = A_1 \exp(-j\theta_1) \qquad \dots (3:3:33)$$

$$\frac{Y_{12}}{Y_0} = A_2 \exp(-j\theta_2).$$
 ...(3:3:34)

First, equation (3:3:34) must be put in more convenient form. Using the expression for Υ_{12} equation (3:3:34) becomes

$$\frac{\lambda_{go}}{\lambda} \left(\frac{\epsilon}{\epsilon_o} - \frac{\mu_o \lambda^2}{\mu_o \lambda_c^2} \right)^{1/2} = A_2 \exp(-j \Phi_2)$$

which when squared is

$$\frac{\lambda_{go}^2}{\lambda^2} \left(\frac{\epsilon}{\epsilon_o} - \frac{\mu_o \lambda^2}{\mu_o \lambda_c^2} \right) = A_2^2 \exp(-j2\theta_2) \qquad \dots (3:3:35)$$

By writing $\epsilon = \epsilon_{o}k_{e}(1-jtan\delta_{e})$ and $\mu = \mu_{o}k_{m}(1-jtan\delta_{m})$ equation (3:3:35) becomes

$$\frac{\lambda_{go}^{2}}{\lambda^{2}} \left(k_{e}(1-j\tan\delta_{e}) - \frac{\lambda^{2}}{k_{m}(1-j\tan\delta_{m})\lambda_{c}^{2}} \right) = A_{2}^{2} \exp(-j2\theta_{2})$$

$$\frac{\lambda_{go}^{2}}{\lambda^{2}} \left(k_{e}\sqrt{1+\tan^{2}\delta_{e}} \exp[-j\tan^{-1}(\tan\delta_{e})] \right)$$

 $-\frac{\lambda^2}{k_m/1+\tan^2\delta_m \lambda_c^2} = \exp\left[j\tan^{-1}(\tan\delta_m)\right] = A_2^2 \exp(-j2\theta_2)$...(3:3:36)

If the loss tangents are such that

$$\sqrt{1 + \tan^2 \delta_e} \stackrel{:}{=} \sqrt{1 + \tan^2 \delta_m} \stackrel{:}{=} 1$$

$$\exp[-j\tan^{-1}(\tan \delta_e)] \stackrel{:}{=} 1 - j\tan \delta_e$$
and
$$\exp[j\tan^{-1}(\tan \delta_m)] \stackrel{:}{=} 1 + j\tan \delta_m$$

equation (3:3:36) becomes

$$\frac{\lambda_{go}^{2}}{\lambda^{2}} \left(k_{e} - \frac{\lambda^{2}}{k_{m}\lambda_{e}^{2}}\right) - j\left(\frac{k_{e}\lambda_{go}^{2}}{\lambda^{2}} \tanh_{e} + \frac{\lambda_{go}^{2}}{k_{m}\lambda_{e}^{2}} \tanh_{m}\right) = A_{2}^{2} \exp(-j2\theta_{2})$$

(3:3) - 45

from which it is evident that

$$A_2^2 = \frac{\lambda_{go}^2}{\lambda^2} k_e - \frac{\lambda_{go}^2}{k_m \lambda_c^2} \qquad \cdots (3:3:37)$$

and

$$2\theta_2 A_2^2 \div \frac{k_e \lambda_{go}^2}{\lambda^2} \tanh_{\theta} + \frac{\lambda_{go}^2}{k_m \lambda_c^2} \tanh_{m}. \qquad ...(3:3:38)$$

By equation (3:3:25) the corresponding equations for the first orientation considered are

$$A_1^2 \doteq \frac{\lambda_{go}^2}{\lambda^2} k_e k_m - k_m \frac{\lambda_{go}^2}{\lambda_c^2} \qquad \cdots (3:3:39)$$

and

$$2\theta_1 A_1^2 \stackrel{!}{=} k_e k_m \frac{\lambda_{go}^2}{\lambda^2} (\tan \delta_e + \tan \delta_m) - \frac{k_m \lambda_{go}^2}{\lambda_c^2} \tan \delta_m \qquad \cdots (3:3:40)$$

If k_e is obtained from equation (3:3:37) and substituted into (3:3:39) the following relation for k_m results:

$$k_{\rm m} = \frac{A_1^2 - \lambda_{\rm go}^2 \Lambda_{\rm c}^2}{A_2^2 - \lambda_{\rm go}^2 \Lambda_{\rm c}^2}$$
 ...(3:3:41a)

ke is then given by

$$k_{e} = A_{2}^{2} - \frac{\lambda^{2}}{\lambda_{go}^{2}} + \frac{\lambda^{2}}{\lambda_{c}^{2}k_{m}}$$
 ...(3:3:41b)

If (3:3:40) is divided by k_{m} and the result subtracted from (3:3:38) tand $_{\rm e}$ may be eliminated thus giving

$$\tanh_{m} \ \ \stackrel{:}{=} \ \ 2 \ \frac{\frac{\theta_{2} A_{2}^{2} - \theta_{1} A_{1}^{2} / k_{m}}{\lambda_{go}^{2}}}{\frac{\lambda_{go}^{2}}{\lambda_{c}^{2}} (1 + \frac{1}{k_{m}}) - \frac{\lambda_{go}^{2}}{\lambda_{2}^{2}} k_{e}} \ \dots (3:3:41c)$$

$$\tanh_{\mathbf{e}} \ \ \div \ \ (2\mathbf{0}_{2}\mathbf{A}_{2}^{2} \ - \ \frac{\lambda_{\mathrm{go}}^{2}}{\lambda_{\mathrm{c}}^{2}\mathbf{k}_{\mathrm{m}}} \ \tanh_{\mathbf{m}}) \frac{\lambda^{2}}{\lambda_{\mathrm{go}}^{2}\mathbf{k}_{\mathrm{e}}} \ . \tag{3:3:41d}$$

v

٠

Experimental Accuracy

4:1 Experimental Errors in the Short circuit - Open circuit Measurements

Because of the complicated calculations involved in determining the electric and magnetic parameters from the measured values of the positions of the first minimum and the standing wave ratios, it is difficult to see what errors result from experimental inaccuracies in these measured values. It has been known, however, that the measurement must be made on samples with lengths of an odd multiple of one-eighth of a wavelength if the results are to be reliable. However, previous to this research no practical procedure for calculating the errors of a measurement has been published. Because of certain simplifying revisions in the formulaes used in the calculation, it was possible to outline such a procedure. This is done in Appendix B.

Since the electric and magnetic parameters for either isotropic or anisotropic media are expressible in terms of A, B, θ and \emptyset , considerable attention will be given to the possible error in these quantities. It is shown in Appendix B that δ B the error in B due to δ X^I and δ X^{II} the errors in the position of the first minimum for the short circuit and open circuit terminations respectively, is given by

$$\delta B = \frac{B\pi}{\lambda_{go}} \left(\frac{\sec^2 \frac{2\pi X^{I}}{\lambda_{go}}}{S^{I}} \delta X^{I} + \frac{\sec^2 \frac{2\pi X^{II}}{\lambda_{go}}}{S^{II}} \delta X^{II} \right)$$

The error in A is shown to be given by

$$\delta A = \frac{1}{Bd(1+v^2)} \left(\sec^2(\frac{2\pi X^{I}}{\lambda_{go}}) \delta X^{I} - v^2 \sec^2(\frac{2\pi X^{II}}{\lambda_{go}}) \delta X^{II} \right) - \frac{b}{d^2} \delta d \quad \bullet$$

The errors, δX^{I} , δX^{II} and δd , are algebraic symbols which may be positive or negative for any particular measurement. It is difficult to see what

order of magnitude these errors will be without giving definite values to k_m , k_a and d and hence determining B, x^I , s^I , x^{II} , s^{II} . However, it is evident that the absolute error in A will in most cases be less than that in B. This is due to the d and d2 in the denominator of the first and second terms of bA. In almost all media of interest the value of A is at least five times greater than that of B and hence the percentage error in A is much less than that in B. To demonstrate this, the errors for A and B have been calculated for a medium having the characteristics of polystyrene $(k_e = 2.52, k_m = 1)$, assuming that $\delta X^{I} = \delta X^{II} = \pm .003$. The estimate of δX was obtained from a consideration of repeated measurements made on a lucite sample, during the course of the work included in this thesis, and it probably represents a maximum error. In Figure 3 the percentage errors in A and B are plotted as a function of the sample length at lengths around two and one-eighth of a wavelength. The plot shows that the percentage error in B is much greater than that in A. Also, the percentage error in B is a minimum at an odd multiple of one-eighth of a wavelength, whereas the percentage error in A decreases slightly as the length is increased. In Figure 4 the percentage errors in kekm, kmand ke are plotted at the same sample lengths. The error in kekm is small since it can be expressed in terms of A alone, whereas in order to calculate $k_{\boldsymbol{e}}$ or $k_{\boldsymbol{m}}$, B must be used.

The expected errors in the loss tangents for such a sample ($tanh_e = .00096$, $tanh_m = 0$) have also been calculated assuming an error in the ΔX 's of $\pm .0003$. The graphs of the absolute error in $tanh_e$ and the percentage error in $\Sigma tanh$ are plotted in Figure 5. It is seen that the error in $tanh_e$ is about 100 percent even at the length corresponding to an odd multiple of one-eighth of a wavelength. However, the error in $\Sigma tanh$ can be as low as 7 percent, which must be considered good for a measurement of a $\Sigma tanh$ of .00096. The reason for this discrepancy is due to the fact that $\Sigma tanh$

Figure 3. Estimated percentage error in A and B for Polystyrene sample at length near 2-1/8 $\lambda_{\mbox{gi}}.$

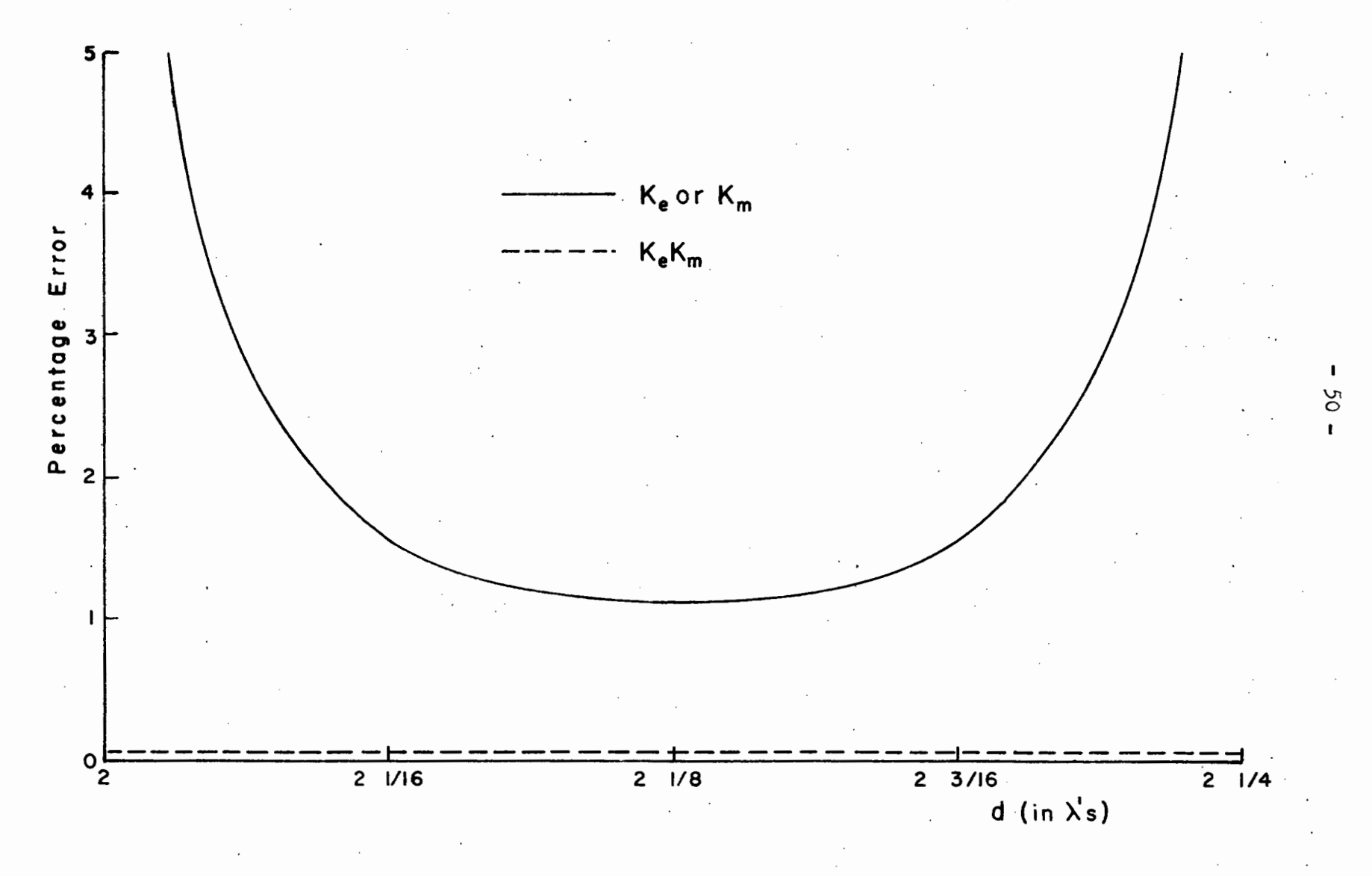


Figure 4. Estimated percentage error in $k_e k_m$, ke and k_m for Polystyrene samples at lengths near 2-1/8 λ_{gi} .

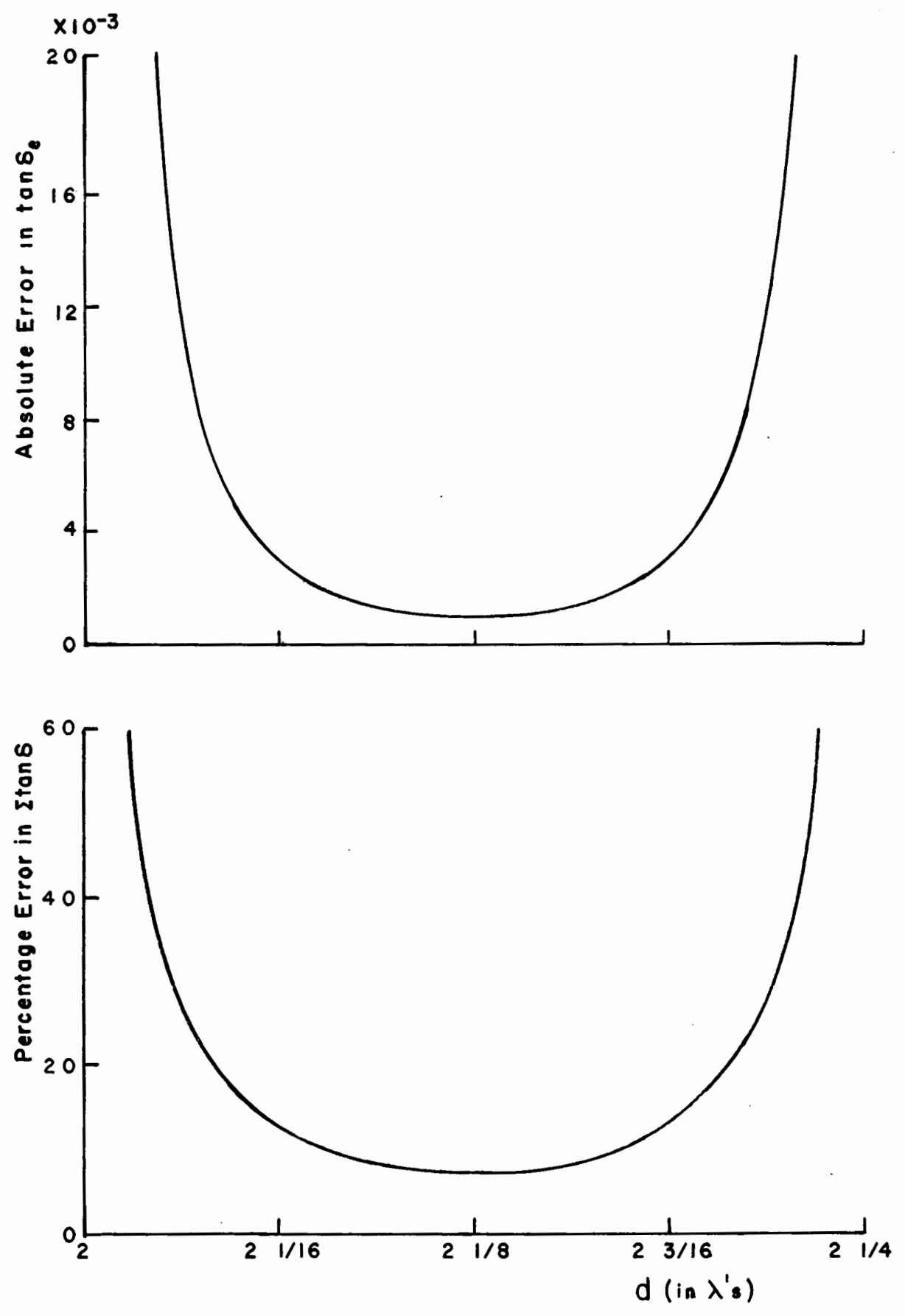


Figure 5. Estimated errors in Ztano and tanoe for Polystyrene samples at lengths near 2-1/8 $\lambda_{\mbox{gi}}$.

can be expressed in terms of Θ and does not involve \emptyset . It is not easy to see why there is a small error in Θ , but the large error in \emptyset is readily evident. For a medium of small losses $\mathbf{T}^{\mathbf{I}}$ and $\mathbf{T}^{\mathbf{II}}$ must be angles which are very nearly equal but opposite in sign. Since, $\emptyset = (\mathbf{T}^{\mathbf{I}} + \mathbf{T}^{\mathbf{II}})/2$, small errors in $\mathbf{T}^{\mathbf{I}}$ and $\mathbf{T}^{\mathbf{II}}$ will result in a large percentage error in \emptyset . For a two and one-eighth wavelength sample the expected error in \emptyset is .0011, whereas that in Θ is only .000042.

Measurements were made on a polystyrene sample of about two and one-eighth wavelengths long. This was done to verify that a measurement could yield results to within the accuracies estimated. The values of the dielectric constant and permeability were in error by 1 percent, whereas the error in the product $k_e k_m$ was negligible. Also while the error in Σ tand was negligible that in tande was 20 percent. These are much less than the estimated errors.

In order to estimate the errors involved in the measurement of the disc array a medium with $k_m=.7500$ and $k_e=4.073$ was considered. The maximum expected errors in A_1 and B_1 are plotted in Figure 6. This shows that at $1-5/8\lambda_{\rm gi}$ the percentage error in B_1 is more than ten times that of A_1 . The general features of the curves are similar to the corresponding ones obtained for the polystyrene sample. The same can be said for the estimated error curves of Θ_1 and \emptyset_1 although these are not plotted. Hence, it may be said that percentage estimated errors in B_1 and \emptyset_1 are comparatively high, those in A_1 and Θ_1 being small.

Since most of the aluminum powder in wax samples were measured at $1-1/8\lambda_{\rm gi}$ it is only necessary that the errors be estimated for a typical sample at that length. For a sample with parameters $k_e=5.000$, $k_m=.900$, $\tan\delta_e=.0000$ and $\tan\delta_m=.0200$, the corresponding estimated absolute

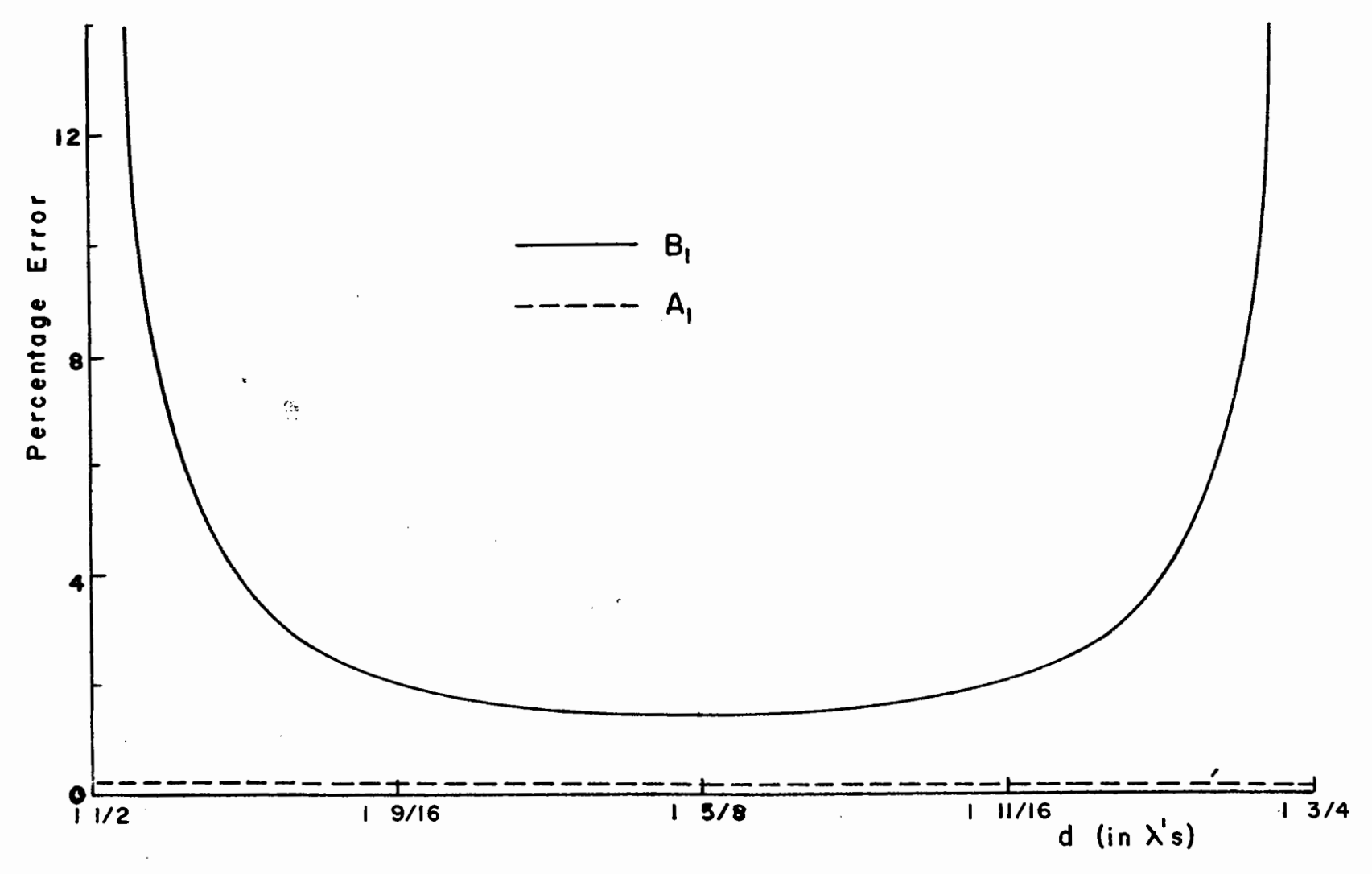


Figure 6. Estimated errors in Al, Bl for a circular disc array for which k_{m} = .7500 and k_{e} = 4.073.

errors are $\pm .030$, $\pm .029$, $\pm .008$ and $\pm .0072$. A larger value of $\delta X(.003)$ is used here, because of the larger error involved in measuring the length of these soft wax samples. It is interesting to notice that since $\delta(\tan \delta_e) = \pm .008$, it is possible for a measurement to yield a negative loss tangent. Negative loss tangents of this order were obtained by Vogan, but were attributed to inhomogeneities in the sample.

In order to give an idea of the deviations in the measured parameters of a given sample the following table lists measurements made on an accurate lucite sample 5/8ths of a wavelength long.

Lucite Sample Σ tan δ $\mathbf{k}_{\mathbf{m}}$ tanb_e $tan \delta_m$ k_e $k_{\mathbf{e}^{\mathbf{k}}\mathbf{m}}$ 2.6268 2.6310 •9986 .00885 -.00055 .00830 2.6110 1.0017 2.6154 .00744 .00010 .00745 2.6395 2.6225 -.00011 **•9935** .00754 .00745 2.6079 1.0027 2.6157 -.00014 .00763 .00775 2.5997 1.0061 2.6156 •00688 .00700 -.00013 2.6034 1.0050 2.6171 .00761 -.00027 .00734 2.5913 1.0069 2.6092 .00681 .00125 .00806 2.5844 1.0078 2.6048 .00036 .00826 .00790 2.5990 1.0086 2.6114 .00780 .00026 .00806 1.0066 2.6083 .00706 .00072 2.5910 .00788 .00758 .00015 .00772 Average 2.6058 1.0038 2.6147 ±.00038 ±.00026 ±.00041 Average $\pm .0132$ ±.0037 ±.0050 deviation

These repeated measurements were made on the same sample over a period of about two years under various conditions. Even for this small length of

sample it is evident that $k_e k_m$ and Σ tand are measured more accurately than the other parameters.

4:2 Accuracy of Semples:-

Preliminary measurements on the aluminum and copper powders did not yield consistent results. For example, the deviation between measurements of km made on two samples which had the same powder content was a much as 30 percent. This inconsistency was thought to be due to inhomogeneities in the samples, which were made by mixing the powder in molten wax until the mixture cooled sufficiently to ensure that the particles Another, and perhaps equally important error was due did not settle out. to the fact that samples could not be cut to the exact dimensions of the guide. A simple but more effective method of making samples was devised which removed inhomogeneities to a large extent and at the same time produced extremely accurate samples. First, a mixture of solid wax and powder was obtained by mixing as described above. A large piece was cut from this and placed in a milling attachment on a lathe. This piece was cut up by the milling tool and the small shavings were collected. The shavings were thoroughly mixed and then firmly pressed into a rectangular hole in a brass block, the dimensions of the hole being the same as the inside dimensions of the waveguide. A tight fitting plunger was made to facilitate the packing which was done on a drill press. The hole was closed off at one end by a plate which could be removed after sufficient packing. sample was removed and placed in the measuring section of the guide. The ends of the sample were cut while it was in the guide. Table 1 gives the results of measurements of a copper powder sample made in this manner. The sample was milled and repacked for each of the four measurements.

Table 1

k _e	k _m	k _e k _m	tanò _e	tanh _m	Σtanδ
2.888	•964	2.785	0009	•0056	.00462
2.928	•943	2.762	•0031	•0010	•00418
2.838	•981	2.785	•0095	0042	•00536
2.930	.956	2.80?	0014	.0059	•00451
2.896	•961	2.784	•0026	.0041	.00467
±.033	±.012	±.010	±.0037	±.0037	±.00035

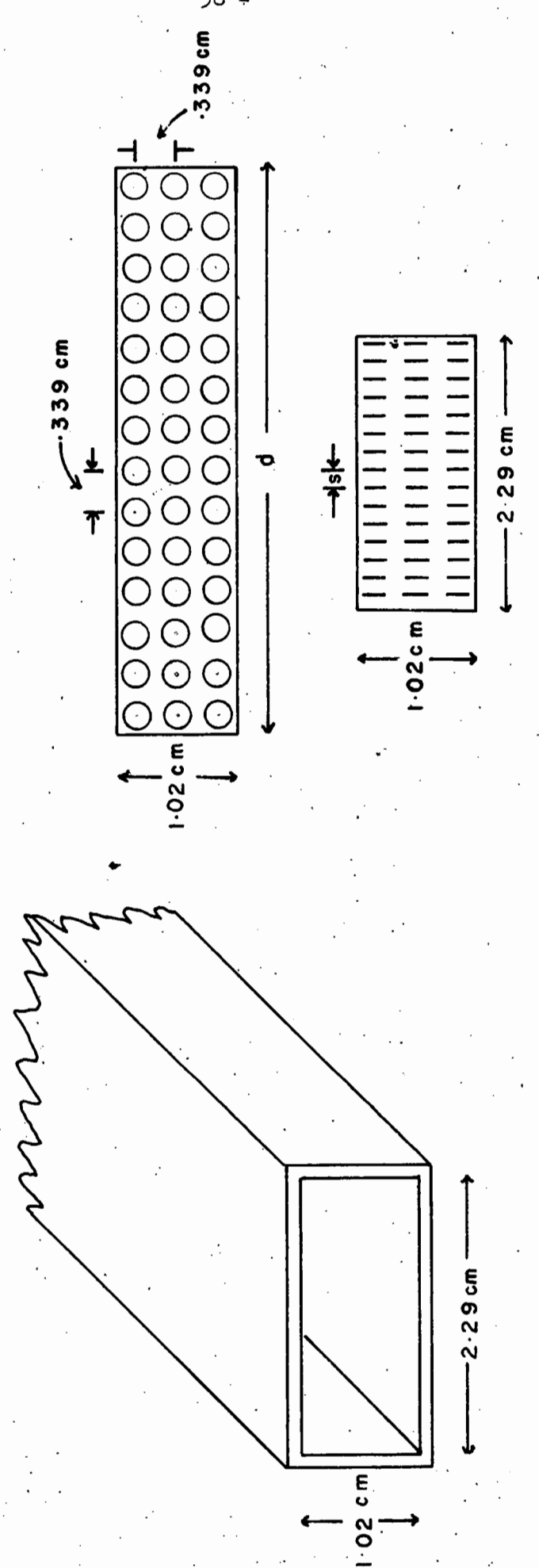
The values of k_e and k_m show only a 1 percent average deviation, that of $k_e k_m$ being about . 4 percent. The results of the measurement of $tanb_e$ and $tanb_m$ are not reliable since the average deviation is of the same order. as the average. The measurements of Σ tanb are fairly consistent however, the percent deviation being only 7.5. Hence, it was concluded that the samples were quite homogeneous, the deviations being of the same order as those caused by inaccuracies in the measurement of the X's and ΔX 's.

A disc array sample was made by placing aluminum discs on wax strips of the same width as the small dimension of the waveguide. The strips had a uniform thickness of 2.08 mms. and eleven strips, placed side by side, formed a sample of the same width as the large dimension of the guide. The discs were pressed slightly into the face of the wax strips to avoid a disarrangement of the lattice structure during the measurements.

In order to investigate disc arrays for which the interaction between discs might be considerable, it was necessary to develop a better method of suspending the discs. First a comparatively long polystyrene sample was made to fit accurately into the measuring section of the guide. A square array of holes each of diameter 2.14 mms. was then drilled in the

sample, the holes being along the length of the sample corresponding to the large transverse dimension of the guide. Figure 7 shows a diagram of this sample. Since the other guide dimension is 1.017 cms., the spacing between the centers of two adjacent holes was made equal to 1/3 of this or .339 cms. The aluminum discs were placed in these holes separated by polystyrene spacers of the same diameter. The discs were produced from aluminum foil sheets by placing the foil sheet on a hard rubber mat and punching out the discs with an accurately machined steel punch. The polystyrene spacers were punched from thin polystyrene sheets through a steel die. The punch and die were set up on a drill press. With polystyrene spacers of different thicknesses the separation between the aluminum discs could be varied. It was found that the average deviation in the thickness of the spacers was as low as one percent. determine the effect of the small air spaces between the spacers, a sample made by merely filling the holes with spacers was measured. For this sample k_e was 2.486 and $tanb_e$ was .00086, whereas for a solid polystyrene sample k_e is 2.519 and $tanb_e$ is .00097. Hence, it was concluded that the spacers were accurately made.

Tong samples were used, since the experimental errors in A_1 and θ_1 are small for such samples. Thus, the time involved in making a sample was considerable. To give an idea of the tedious tork involved, one sample containing 45 holes required about 3600 discs and spacers.



Sample Dimensions

Waveguide Dimensions

Figure 7.

Chanter 5

Experimental Results

5:1 Aluminum and Copper Powders in Wax

The results of the measurements made on the samples of thick aluminum and copper particles in wax are given in Table $2 \cdot$

Table 2

2a Aluminum 66 - 444

Sample Length	k m	^k e	k _e	$\mathtt{tanb}_{\mathtt{m}}$	tanò _e	Σtanδ
1-1/8 λ_{gi}	•899	5.022	2.232	•022	•005	•0264
1-1/8 \(\lambda_{\text{gi}}\)	•910	5.050	2.244	.022	•004	.0261
1-1/8 \(\lambda_{\text{gi}}\)	-920	5.000	2.222	.016	.009	.0255
1-3/8 \(\lambda_{\mathref{gi}}\)	•925	4•993	2.219	.018	. 008	.0262
Average values	•911	5.016	2.229	•020	•006	.0261
Average deviatio	n±.009	±.020	±.009	±.002	±.002	±.0003

2b Aluminum 177 - 1494

Sample Length	k _m	^k e	ıı k e	$ an\delta_{ ext{m}}$	tanò _e	Σtanδ
7/8 λ _{gi}	.924	5.02	2.23	.020	003	.0170
1-1/8 \(\lambda_{\text{gi}}\)	•923	5.10	2.27	.027	009	.0174
1-1/8 \(\lambda_{\text{gi}}\)	•964	4.87	2.16	•012	.005	.0165
$7/8~\lambda_{\rm gi}$.873	5.27	2.34	.018	002	.0158
Average values Average	.921	5.07	2.25	•019	002	•0166
deviation	±.024	±0.12	±.05	±.004	±.004	±.0005

2c Aluminum 500 - 350H

Sample Length	k _m	^k e	k _e	$ an\delta_{ exttt{m}}$	tanò _e	∑tanò
1-3/8 \(\lambda_{\text{gi}}\) 1-3/8 \(\lambda_{\text{gi}}\) 1-3/8 \(\lambda_{\text{gi}}\) 1-1/8 \(\lambda_{\text{gi}}\)	•917 •898 •988 •968	3.90 3.94 3.59 3.67	1.73 1.75 1.60 1.63	.0045 .0064 .0060	.0007 .0012 0008 0003	.00520 .00517 .00608 .00481
Average values Average deviation	•943 ±. 035	3.78 ±.14	1.68 ±.07	.0055 ±.0007	.0002 ±.0007	.00532 ±.00039

2d Copper 500 - 350µ

Sample Length	k _m	^k e	k _e	tanò _m	tanò _e	Σtanδ
1-1/8 \(\lambda_{\text{gi}}\)	•964	2.89	1.28	•0056	0009	•00462
1-1/8 λ _{gi}	•943	2.93	1.30	.0010	•0031	.00418
1-1/8 λ_{gi}	•981	2.84	1.26	0042	•0095	.00536
1-1/8 λ _{gi}	•956	2•93	1.30	•0059	•0014	•00451
Average values Average deviation	.961 ±.012	2.90 ±.03	1.285 ±.013	.0041 ±.0037	.0026 ±.0037	.00467 ±.00035

k_e is the dielectric constant of the particles alone and is obtained by dividing the measured dielectric constant by that of the wax, which is 2.25. The notation 500-350 microns refers to the range of dimensions of the particles. This range was obtained by first sifting powder through a 500 micron screen and then sifting out the smaller particles through a 350 micron

(5:1) - 61 -

Limited. No attempt was made to determine the exact particle thicknesses, but an examination of the particles under a microscope indicated that the ratio of thickness to diameter was of the order of one-twentieth for both aluminum and copper particles. Hence, the particles were flake-like, resembling discs more than any other simple geometrical figure, but generally they were of completely irregular outline. Each sample contained roughly .07 gms. of metal per cc. It is noted that in each case the measurements were made at sample lengths near an odd multiple of one-eighthof a wavelength in the dielectric filled guide. It was assumed that the particles were randomly oriented in which case the analysis pertaining to isotropic media was used to obtain the parameters from the measured values of the positions of the minima and the standing wave ratios.

A comparison of these results with the values predicted by the No-interaction theory is easily made by examining the experimental value of the ratio

$$\frac{1-k_{m}}{k_{e}^{m}-1} = -\frac{N\alpha_{m}}{N\alpha_{e}} = -\frac{\alpha_{m}}{\overline{\alpha_{e}}}$$

This is actually the ratio of the magnetic to electric susceptibility. Since, for circular discs $\alpha_m = -\frac{8}{3} \, \mathrm{R}^3$ and $\alpha_e = \frac{16}{3} \, \mathrm{R}^3$ this ratio is .5 and is independent of the size distribution of the particles. A somewhat similar ratio is available which serves to compare experimental results with the Clausius-Mossotti equation. This ratio is

$$\frac{(1-k_m)/(k_m+2)}{(k_e^n-1)/(k_e^n+2)} = -\frac{\alpha_m}{\alpha_e}$$

which again, according to theory, is .5. In Table 3 the experimental values of these ratios are given for the four samples measured.

Table 3

Sample	Experimental value of $\frac{1-k_m}{k_e^{"}-1}$	Experimental value of $\frac{1-k_{m}}{k_{m}+2} / \frac{\frac{k''-1}{e}}{\frac{e}{k''+2}}$
Al. 66-44	•145	.106
Al. 177-149	.127	.092
Al. 500-350	•084	•105
Cu. 500-350	•272	•151

In each case the ratio is much less than predicted by theory. It should be noted, however, that the theoretical values of these ratios do not take into consideration the fact that the particles are randomly oriented. A glance at equation (2:2:1) makes it evident that

$$\frac{1-k_{m}}{k_{e}^{n}-1} = -\frac{1}{2} \frac{\alpha_{m}}{\alpha_{e}} = .250$$

for discs which are randomly oriented. It is also easily shown that

$$\frac{(1-k_{\rm m})/(k_{\rm m}+2)}{(k_{\rm e}''-1)/(k_{\rm e}''+2)}$$

also equals .250 if the Clausius-Mossotti equations apply. Nevertheless, it is evident that in general the agreement between experiment and theory is poor. If the particles making up the dielectric are generally of more elongated shapes, the theoretical values of the ratios will be smaller since α_m is less than one-half α_e for such particles. In this case better agreement with experiment would be expected.

From this investigation it must be concluded that a complete explanation of the small diamagnetic effect in the aluminum samples must be applicable to particles with thicknesses much greater than skin depth.

The experimental values of the tand's serve only to confirm the findings of E.L. Vogan, namely, that the greater part of the loss is associated with the circulating currents in the particles rather than with the electric polarization effect.

5:2 Aluminum Disc Array in Wax

In order to understand completely the phase delay property of the aluminum powder dielectrics, it is necessary that the small diamagnetic effect be explained. The main difficulty in a quantitative interpretation of the results of the metal powder measurements arises from the fact that the size and separation of the particles vary over wide ranges. An investigation of the electric and magnetic properties of a regular array of disc obstacles of uniform size and separation should yield information which could be more easily interpreted. If the lattice dimensions are large, the interaction is small and the expressions for the polarizabilities can be checked. Also, if the lattice dimensions are varied the interaction between the discs can be investigated. The first investigation was carried out on a sample of discs supported in wax as described in Chapter 4 and the latter will be considered in the next section. The sample was oriented in the guide with the discs parallel to the propagation direction such that its electric and magnetic properties could be represented by the tensors

$$(\epsilon) = \begin{pmatrix} \epsilon_0 & 0 & 0 \\ 0 & \epsilon & 0 \\ 0 & 0 & \epsilon \end{pmatrix} \quad \text{and} \quad (\mu) = \begin{pmatrix} \mu & 0 & 0 \\ 0 & \mu_0 & 0 \\ 0 & 0 & \mu_0 \end{pmatrix}$$

and the values of the tensor commonents were obtained from the positions of the minima and the standing wave ratios through equations (3:3:22),(3:3:23), (3:3:27) and (2:3:28).

The diameter of the aluminum foil discs was 2.13 mms.and S, the separation between adjacent planes containing the discs was 2.08 mms. The number of particles per cubic cm. was 55.4. The results of 18 measurements taken at different sample lengths are given in Table 4.

Table 4

Sample length cms.	$k_e^{k_m}$	k _m	k _e	tanòm	tanò _e	Σtanδ
2.3943 2.3868 2.4208 2.4492 2.5184	2.5430 2.5642 2.5659 2.5733 2.6165	•757 •771 •7941 •8128 •8892	3.3593 3.3258 3.2312 3.166 2.9425	.0024 .0025 .0016 .0013 .00324	00077 00076 00003 +.00012 00153	.00163 .00174 .00157 .00142
2.5512 2.5715 2.5951 2.6500 2.8077	2•5555 2•5632 2•5487 2•6056 2•5773	.7651 .817 .776 .8964 .8340	3.3401 3.1373 3.2844 2.9067 3.0903	.0013 .0037 .0016 .0077 0013	+.00015 0020 00016 00528 +.00209	.00143 .00170 .00144 .00242 .00079
2.8357 2.8730 2.9058 2.9528 2.9964	2.5976 2.5715 2.6171 2.5327 2.5844	.8745 .8301 .0736 .7197 .7990	2.9704 3.0978 2.9958 3.5191 3.2345	00328 0007 0022 0009 0052	+.00385 +.00195 +.00304 +.00224 +.00618	.00057 .00125 .00084 .00215
3.0622 3.4882 3.9187	2.5709 2.6325 2.601	•7765 •8914 •7927	3.3109 2.9532 3.2812	00825 .00062 0041	+.00882 +.00073 +.00490	.00057 .00135 .00090
Average	2.583	.821	3.159			.00135

The percentage deviations from the mean value of k_m are plotted in Figure 8. It is seen that the deviation is as much as 10 percent for some of the measurements. While some experimental errors due to errors in the measurement

Figure 8. Percentage deviation from the mean of the measured values of \mathbf{k}_m for an aluminum disc array supported in wax.

of the X's and E's are present, it is obvious from the discussion of errors in the previous chapter that such large deviations must have a different origin. These irregular variations have been observed by Corkum for an array of spherical obstacles. He assumed that they are due to a difference in the actual physical length and the "effective" length of the sample. That is, the refractive index of these obstacle type artificial dielectrics increases from unity to the true or bulk value through a transition region. Two samples, one an artificial, the other a natural dielectric, which have the same bulk refractive index as well as the same total phase delay, in general will not be the same physical length. The length of this ordinary dielectric sample is termed the effective length of the artificial dielectric sample. Corkum⁸ observed that although the percent deviations in k_e and k_m were large the values of the product $k_e k_m$ were constant. This may be explained by the discussion of errors carried out in the previous chapter. A large error in the length of the sample will cause large errors in the quantities X and X. These errors will cause a large error in B, but only a comparatively small error in A. Corkum's sphere array was isotropic the product kekm can be expressed in terms of A alone and hence, the error in this product will be comparatively small.

Recalling that for a disc array in which the discs are parallel to the direction of propagation along the guide

$$A_1^2 = \frac{\lambda_{go}^2}{\lambda^2} \left(k_e k_m - k_m \frac{\lambda}{\lambda_c^2} \right)$$

it is evident that even in this anisotropic case there will be a small

percentage error in kekm. This is because of the fact that the second term is always small compared to the first. For example, in this case λ^2/λ_c^2 = .4877 and k_m = .820, the reas $k_e k_m$ = 2.58. Hence, the comparatively large error in the second term due to the fact that B must be used to determine k_{m} will have little effect and the error in $k_{e}k_{m}$ will result principally from the error in A1. By examining the complex part of ecuation (3:3:25), similar reasoning will lead to the conclusion that $\Sigma an\delta$ will have a smaller error than those associated with tende or tank m. By reference to the results in Table 4 it is seen that the values of the product kekm and 2 tand are much more consistent than those of the other nerameters. Actually, the deviations in tande and tand are so large that it is not logical to average the results. However, those in the other parameters are not too large and the average values have meaning. Since the permittivity of the medium is equal to that of the supporting medium multiplied by that of the obstacles 1, it can be shown that the electric loss due to the discs is equal to the total loss minus that of wax. tande is .00038 for wax, hence the total loss due to the discs is. 00097. In Table 5 the average of the experimental values of $k_e k_m$, k_e and k_m are compared with the Clausius-Mossotti and the No-interaction values.

Table 5

Experimental			Clausius-Mossotti			No-interaction		
k _e k _m	k _e	k _m	k _e k _m	k e	k _m	k _e k _m	^k e	k _m
2.582	3.16	0.821	2.56	3.16	0.811	2.51	3.05	0.822

Since the product NC is small for this particular sample, the difference

between the two theoretical values for each parameter is slight and it is impossible to tell which of the two best describes the experimental results. Certainly the agreement between experiment and theory is as good as can be expected. Because of this it must be concluded that the electric and magnetic polarizabilities serve to describe the properties of a disc array when the interaction is small. Herce, any theoretical investigation of the properties of an individual disc, for example, an attempt to extend the results of Estrin's theory to include the effect of the finite conductivity of the disc, should not alter the expression for the real part of polarizability.

5:3 Aluminum Disc Arrays in Polystyrene

From the research carried out on the thick aluminum and copper powders it was learned that permeabilities only slightly less than unity are observed for thick as well as thin particles. This, along with the results just obtained, makes it possible to conclude that a satisfactory explanation of this small magnetic effect cannot be acquired through a more critical examination of the magnetic polarizability of a single particle. Hence, by a process of elimination it appeared that the explanation might have its origin in the interaction between the particles.

In order to investigate the effect of the interaction experimentally, five samples of aluminum disc arrays supported in polystyrene were made as described in Chapter 4. The diameter of each disc was 2.14 mms., the distance from the center of a disc to the center of a nearest neighbour in its own plane was 3.39 mms. S, the spacing between adjacent planes containing the disc faces was different for each sample and was as small as 0.55 mms. for one sample. Table 6 gives the results of such measurements made on a sample for which the spacing was .852 mm.

Table 6

Sample Length cms.	k _e k _m	k _m	k _e	∑tanò	tanò _e	tanb _m
2.7753	2.875	.6714	4.519	.00190	.00347	00157
3.6281	2.898	.6881	4.211	.00335	00723	.01058
3.6454	2.877	.6901	4.169	.0052	0195	.0247
3.6654	2.893	.6995	4.136	.00363	00753	.01116
3.6810	2.893	.7082	4.085	.00354	00661	.01015
3.6933	2.868	.7042	4.101	.00402	00901	.01303
3.7067	2.893	.7103	4.073	.00456	01136	.01592
3.7199	2.895	.7153	4.047	.00466	01211	.01697
3.7332	2.895	.7172	4.036	.00520	01292	.01812
3.7607	2.894	.7150	4.047	.00576	01557	.02133
3.7858 3.8067 3.8191 3.8472 3.8821	2.877 2.879 2.889 2.860 2.833	.7030 .6900 .7011 .6547 .5934	4.106 4.173 4.121 4.368 4.774	.00551 .00481 .00399 .00378 .00347	01407 01123 00672 00397 00567	.01958 .01604 .01071 .00775
3.9129	2.872	.6362	4.514	.00230	.00337	00107
3.9334	2.875	.6568	4.378	.00248	00016	.00264
3.9413	2.914	.7342	3.969	.00228	.00093	.00135
4.2354	2.853	.6271	4.550	.00278	00436	.00714
4.2371	2.890	.7005	4.125	.00372	00435	.00807
4.2411	2.935	•7059	4.105	.00364	00557	.00921
4.2607	2.848	•6123	4.651	.00358	00493	.00851
4.2629	2.850	•6221	4.582	.00335	00260	.00595
4.2700	2.847	•6167	4.617	.00353	00345	.00698
4.2773	2.851	•6152	4.634	.00330	00191	.00521
4.2842	2.849	.6133	4.646	.00288	.00017	.00271
4.3125	2.988	.8847	3.377	.00325	00394	.00719
4.3347	2.974	.8620	3.450	.00361	00578	.00939
4.3483	2.971	.8524	3.485	.00377	00703	.01080
4.3995	2.939	.7922	3.710	.00203	00029	.00232
4.7493	2.886	.6860	4.207	.00280	00197	.00477
4.7493	2.885	.6743	4.278	.00303	00209	.00512
4.7511	2.878	.6666	4.318	.00237	00051	.00288
4.7511	3.040	.6870	4.425	.00187	.00324	00137
5.1038	3.043	.9241	3.293	.00000	.0127	0127

There are large variations in the measured values of all quantities except $k_e^{}k_m^{}$ and $\lambda tanb$. In Figure 9 the percent deviation of $k_m^{}$ is plotted at several sample lengths and it is shown that this deviation is as high as 20 percent. From this it is evident that errors associated with the transition region of the array are larger than those encountered in the previous investigation. This is to be expected since there are a greater number of discs near both interfaces of the sample. To give added weight to the assumption that the interface problem is of considerable importance, graphs of the variation of the parameters with sample length for several lengths near 1-7/8 λ_{gi} are given in Figure 10. Originally the sample was 1-15/16 wavelengths long and measurements were taken as it was milled to a length slightly less than 1-13/16 $\lambda_{\sigma i}$. The diagram of the sample serves to indicate the positions of the discs relative to the physical interface. As the length is changed by small amounts the values of the parameters change only slightly and in a continuous manner. This is to be expected for when the length is changed slightly the corresponding change in the difference between the effective and physical length is small. The discontinuous variations occur only when the sample length is altered a great deal, for example from 2-1/8 to 1-7/8 λ_{gi} . Changes of this sort, of course, in general would seriously alter the discrepancy between the effective and actual length since the diameter of the discs is of the order of $1/8 \lambda_{gi}$.

It has been noted that experimental errors in the measured values of the positions of the first minima and the standing wave ratios produce comparatively large errors in B_1 and \emptyset_1 , those in A_1 and Θ_1 being small. To illustrate this, the values of A_1 , B_1 , \emptyset_1 and Θ_1 are given in Table 7.

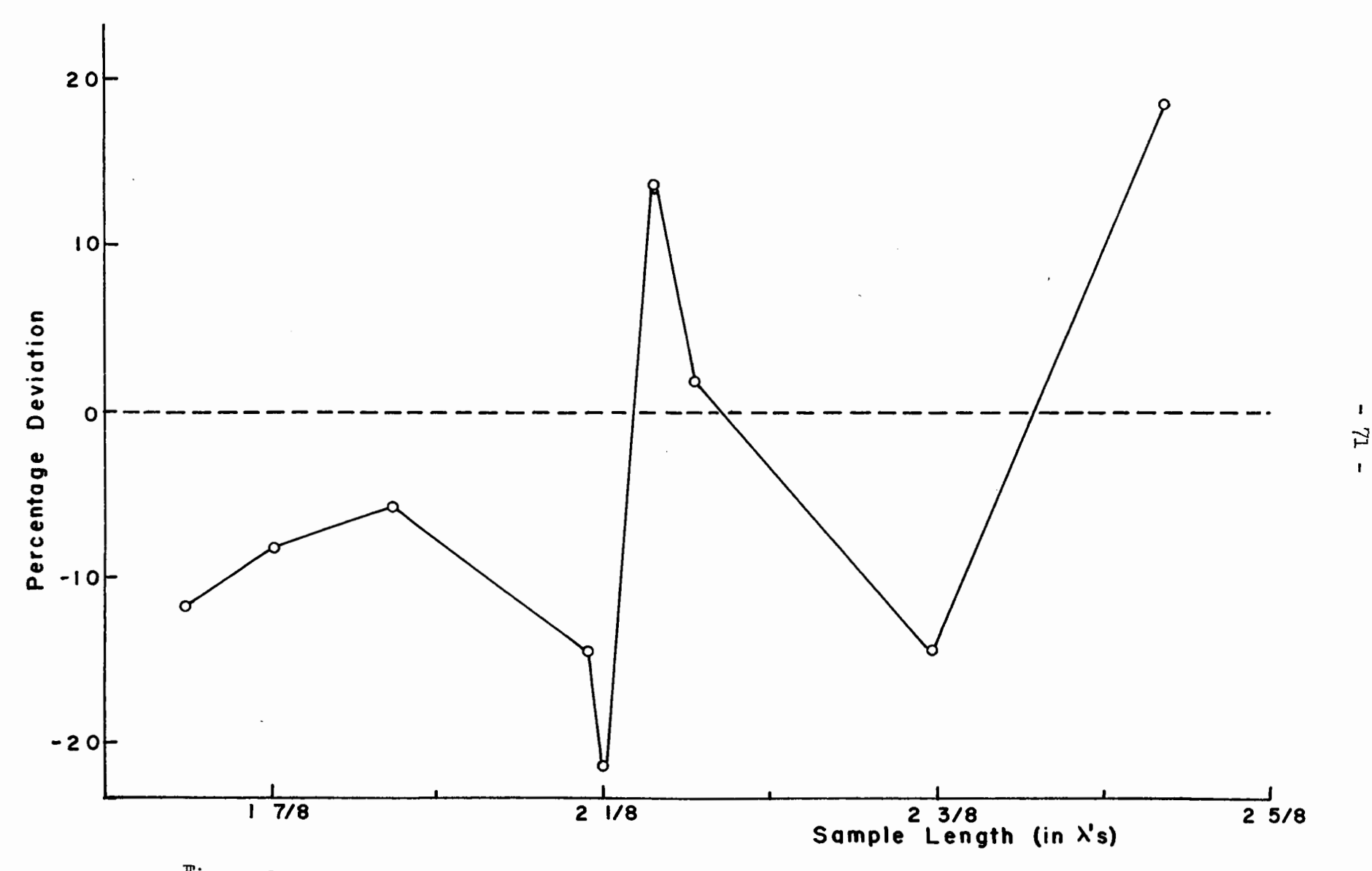


Figure 9. Percentage deviation from the mean of the individual values of k_m for an aluminum disc array for which $S=.852\ mm$.

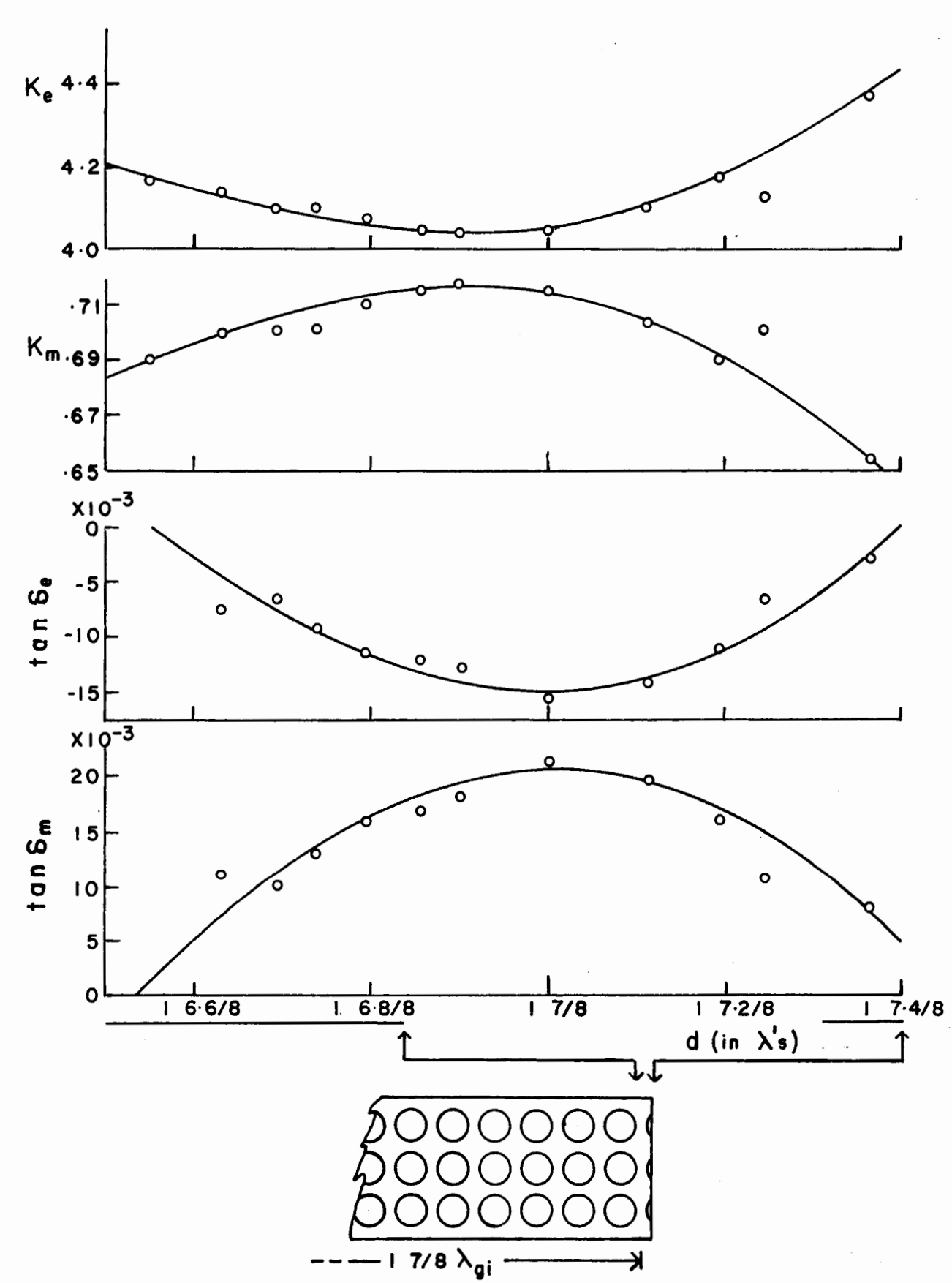


Figure 10. Variation of the measured electric and magnetic parameters of an aluminum disc array with sample length.

Table 7

Sample Length (cms.)	B ₁	ø ₁	A ₁	θ ₁
2.7753	•3012	.0028	2.2292	.00123
3.6281	•3077	0118	2.2363	.00125
3.6454	•3099	0113	2.2267	.00134
3.6654	•3134	0098	2.2319	.00136
3.6810	•3176	0088	2.2298	.00138
3.6933	.3160	0116	2.2286	.00146
3.7067	.3186	0144	2.2293	.00157
3.7199	.3208	0153	2.2293	.00167
3.7332	.3218	0163	2.2287	.00178
3.7607	.3208	0194	2.2289	.00189
3.7858	•3155	0177	2.2281	.00188
3.8067	•3097	0143	2.2279	.00174
3.8191	•3144	0091	2.2299	.00161
3.8473	•2940	0060	2.2269	.00173
3.8821	•2663	0076	2.2284	.00151
3.9129 3.9334 3.9413 4.2354 4.2371	.2849 .2941 .3287 .2812 .3141	.0025 0014 0001 0060 0064	2.2332 2.2334 2.2335 2.2299 2.2302	.00143 .00129 .00125 .00119
4.2411	•3162	0077	2.2325	.00151
4.2607	•2745	0069	2.2305	.00159
4.2629	•2790	0043	2.2296	.00161
4.2700	•2766	0053	2.2294	.00165
4.2773	•2757	0036	2.2313	.00163
4.2842	.2749	0012	2.2311	.00154
4.3125	.3961	0059	2.2336	.00131
4.3347	.3861	0080	2.2325	.00135
4.3483	.3817	0095	2.2331	.00134
4.3995	.3549	0010	2.2323	.00137
4.7493	.3074	0034	2.2316	.00133
4.7493	.3019	0036	2.2335	.00145
4.7511	.2986	0017	2.2323	.00121
4.7511	.3078	.0026	2.2320	.00120
5.1038	.4206	.0099	2.2312	.00119
Average Average deviation	•3143 ±.024	.0066 ±.0050	2.2306 ±.0018	.00143 ±.00017

(5:3) - 74 -

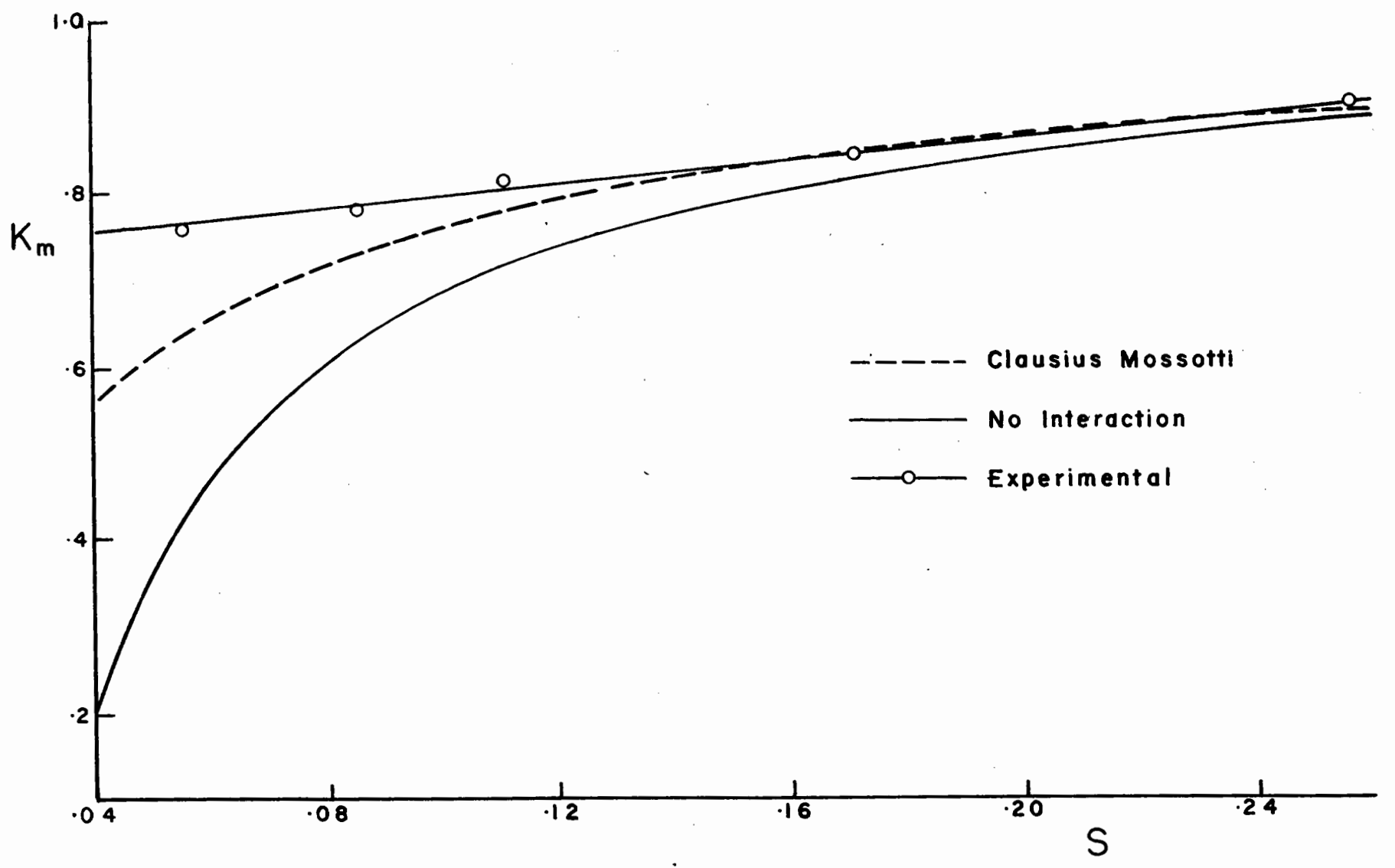
Because of this interface difficulty the average values of the parameters do not have much meaning. However, if the sample is oriented in the guide with the disc faces perpendicular to the propagation direction, the permittivity and permeability tensors become

$$(\epsilon) = \begin{pmatrix} \epsilon & 0 & 0 \\ 0 & \epsilon & 0 \\ 0 & 0 & \epsilon \end{pmatrix} \qquad (\mu) = \begin{pmatrix} \mu_0 & 0 & 0 \\ 0 & \mu_0 & 0 \\ 0 & 0 & \mu \end{pmatrix}$$

and the second analysis of anisotropic media considered in Chapter 3 applies. Measurements were made on this sample for such an orientation and the electric and magnetic parameters were obtained from the two sets of values of A and Θ . The pertinent relations are given in equations (3:3:41). It is noted also in Chapter 3, that the theoretical value of the product A_2B_2 should be exactly unity. The average experimental value was .99 \pm .05. Better agreement could not be expected because of the large errors in the values of B_2 . The average values of A and Θ are $A_1 = 2.2306$, $\Theta_1 = .00143$, $A_2 = 2.4763$ and $\Theta_2 = .00091$, and when substituted into equations (3:3:41) the following values of the electric and magnetic parameters are obtained:

$$k_{m} = .779$$
, $ten \delta_{m} = .00137$
 $k_{e} = 3.768$, $tan \delta_{e} = .00129$.

The results of similar measurements made on four other samples are given in Table 8. The A's and Θ 's represent averages of values obtained from several measurements for each of the two orientations. In Figure 11, the experimental values of k_m are compared with those predicted from the No-interaction and Clausius-Mossotti equations. Both agree with experiment at the larger spacings. This is to be expected since at these spacings the interaction between aiscs is negligible.



75

Figure 11. The permeability of aluminum disc arrays as a function of the spacing between the disc faces.

Table 8

Spacing between discs	A ₁	A ₂	0 1	9 2	k _e	k _m	tanò _e	t an δ_{m}
0.055	2 . 29 71	2•5858	•00167	.00101	4.073	•754	•00142	.00173
0.110	2.2080	2.4101	.00137	.00093	3.580	.80 8	.00135	.00119
0.171	2.1326	2.2866	.00105	•00090	3.259	.841	.00139	.00047
0.256	2.0822	2.1667	.00075	.00075	2.945	•904	•00123	0004

At the smaller spacings, however, the experimental differ markedly from theoretical values. It should be pointed out that at these separations the lattice structure is far from cubic and the lattice structure correction terms, A_x , A_y , A_z , mentioned in the theory in connection with the Clausius-mossotti equation are not negligible. In any case, these experimental results indicate that the permeability effect is small when the discs are closely packed.

In Figure 12 the experimental values of the dielectric constant are compared with the corresponding No-interaction and Clausius-Mossotti values. Again the agreement is good at the larger disc separations, the experimental values being smaller for the densely packed arrays. These experimental values of the dielectric constant are in agreement with the static values of S.B.Cohn obtained by the electrolytic method. He found that the measured dielectric constant was lower than theoretical values when the ratio of the separation between discs to the distance between adjacent discs in the same plane was less than 75.

In an attempt to give theoretical confirmation to the experimental

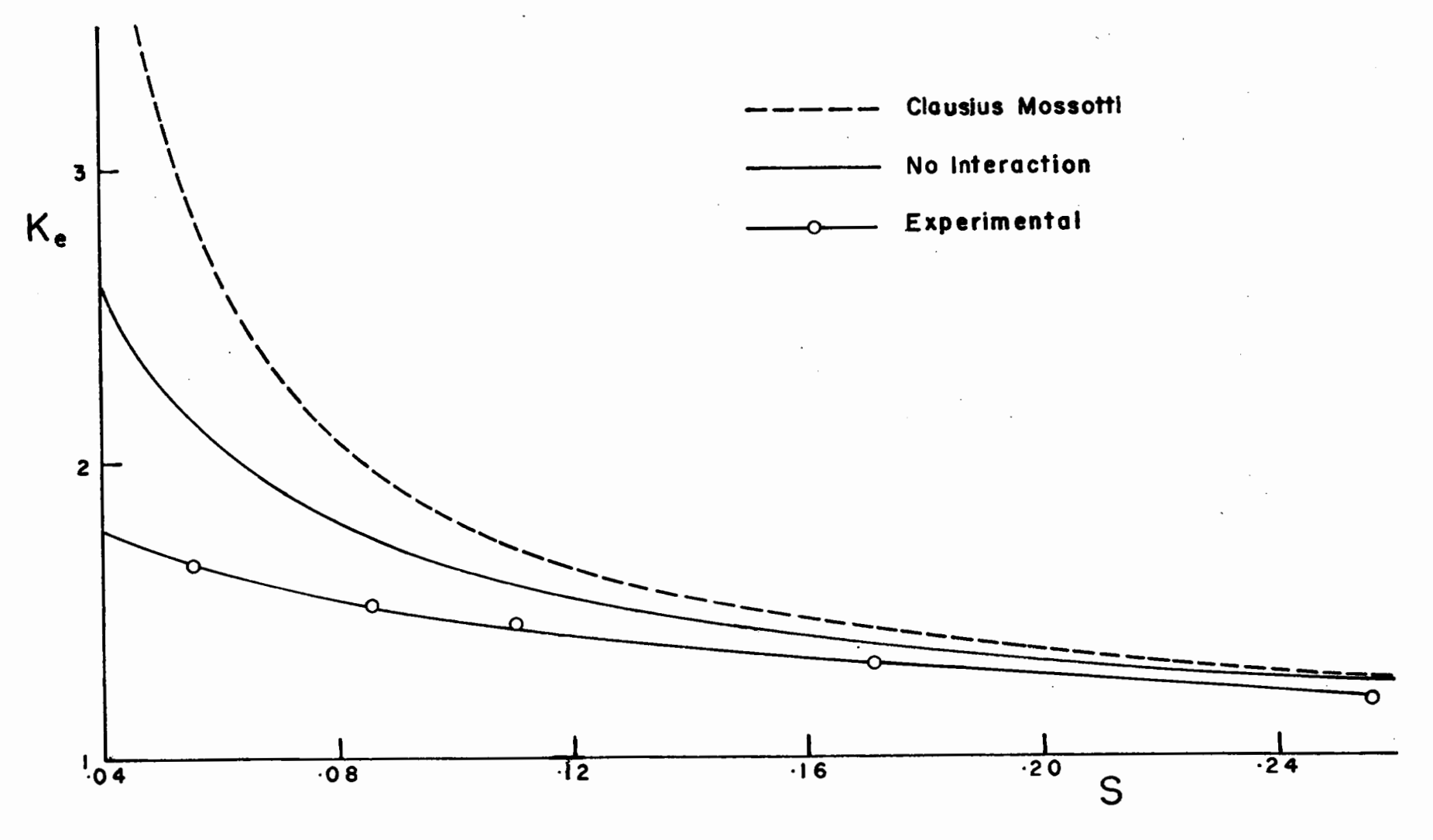


Figure 12. The dielectric constant of aluminum disc arrays as a function of the spacing between the disc faces.

values of k_e and k_m , the lattice structure correction terms A_x , A_y and A_z were obtained by numerical calculation for two rectangular lattices. When the disc faces are parallel to the xy plane the apparent electric and magnetic polarizabilities are given by

- 78 -

$$\frac{1}{\beta_{\text{ex}}} = \frac{1}{\beta_{\text{ey}}} = \frac{1}{\alpha_{\text{ex}}} + A_{x} \qquad \dots (5:3:1a)$$

$$\beta_{ez} = \beta_{mx} = \beta_{my} = 0$$
 ...(5:3:1b)

$$\frac{1}{\beta_{mz}} = \frac{1}{\alpha_{mz}} + A_z \qquad ...(5:3:1c)$$

One of the rectangular lattice structures considered was that for which the x and y lattice distances were .339 cm., the z distance being .200 cm. The constant

$$A_{z} = \frac{1}{4\pi} \sum_{k} \frac{1}{r_{k}^{3}} \left(1 - \frac{3z^{2}}{r_{k}^{2}}\right)$$

obtained by summing over all lattice points in a Lorentz sphere of radius 1.695 cms is equal to -35.23 cm⁻³. Also, it was shown that $A_{\rm X} = A_{\rm Y} = -1/2$ $A_{\rm Z}$. The effective polarizabilities were then obtained from equations (5:3:1) and inserted into the Clausius-Mossotti expression. The dielectric constant and permeability obtained in this way are 1.320 and .866 respectively. If the actual polarizabilities are used the values are $k_{\rm e}^{\rm H} = 1.352$ and $k_{\rm m} = .850$. The modified equation predicts a lower dielectric constant and a higher permeability. This is true in general for this type of lattice if S is smaller than .339 cm. Also, as the spacing is decreased $A_{\rm Z}$ becomes larger in absolute value and the discrepancies between the values predicted by the effective and actual polarizabilities become greater. Experimentally

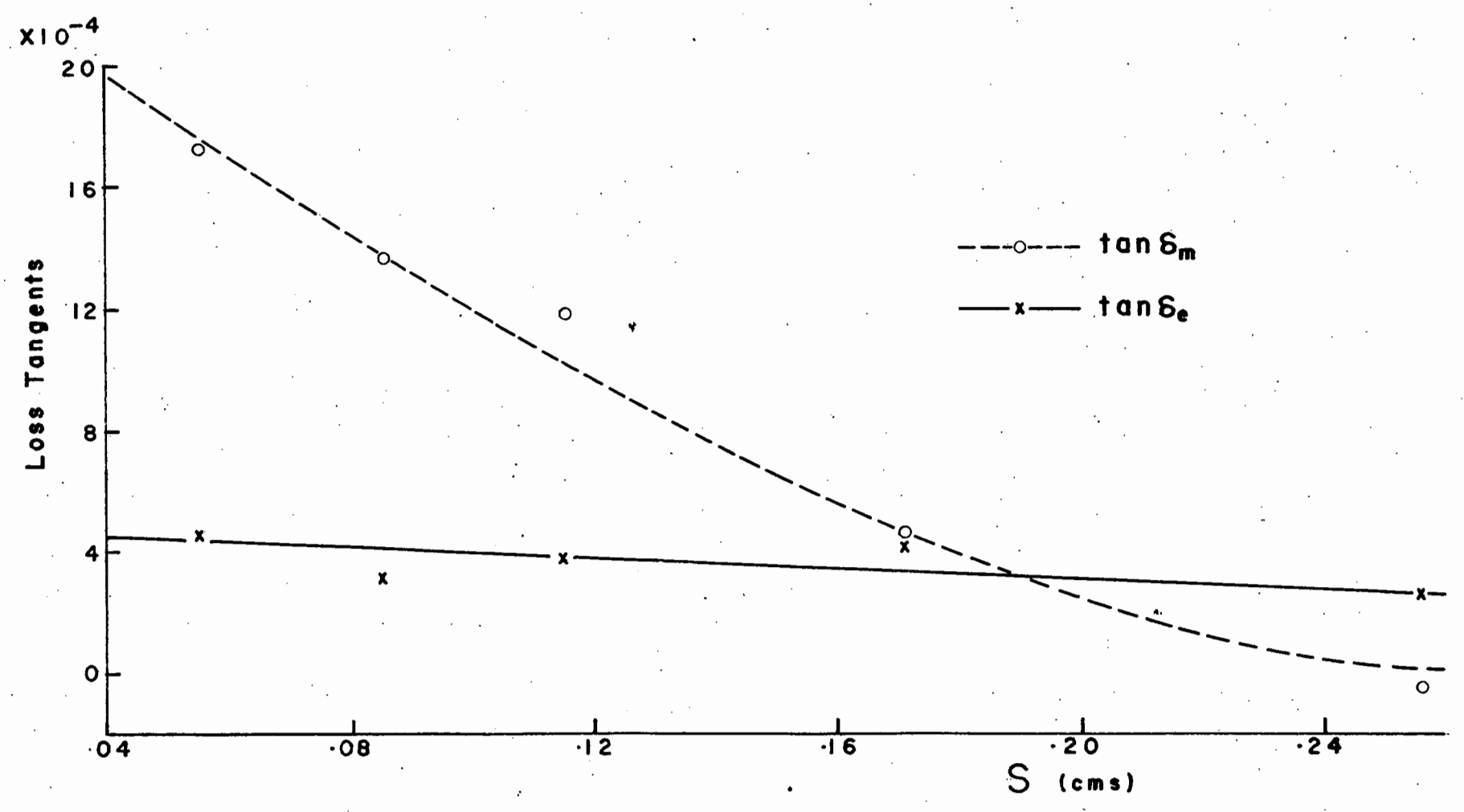


Figure 13. The electric and magnetic loss tangents as a function of the spacing between the disc faces.

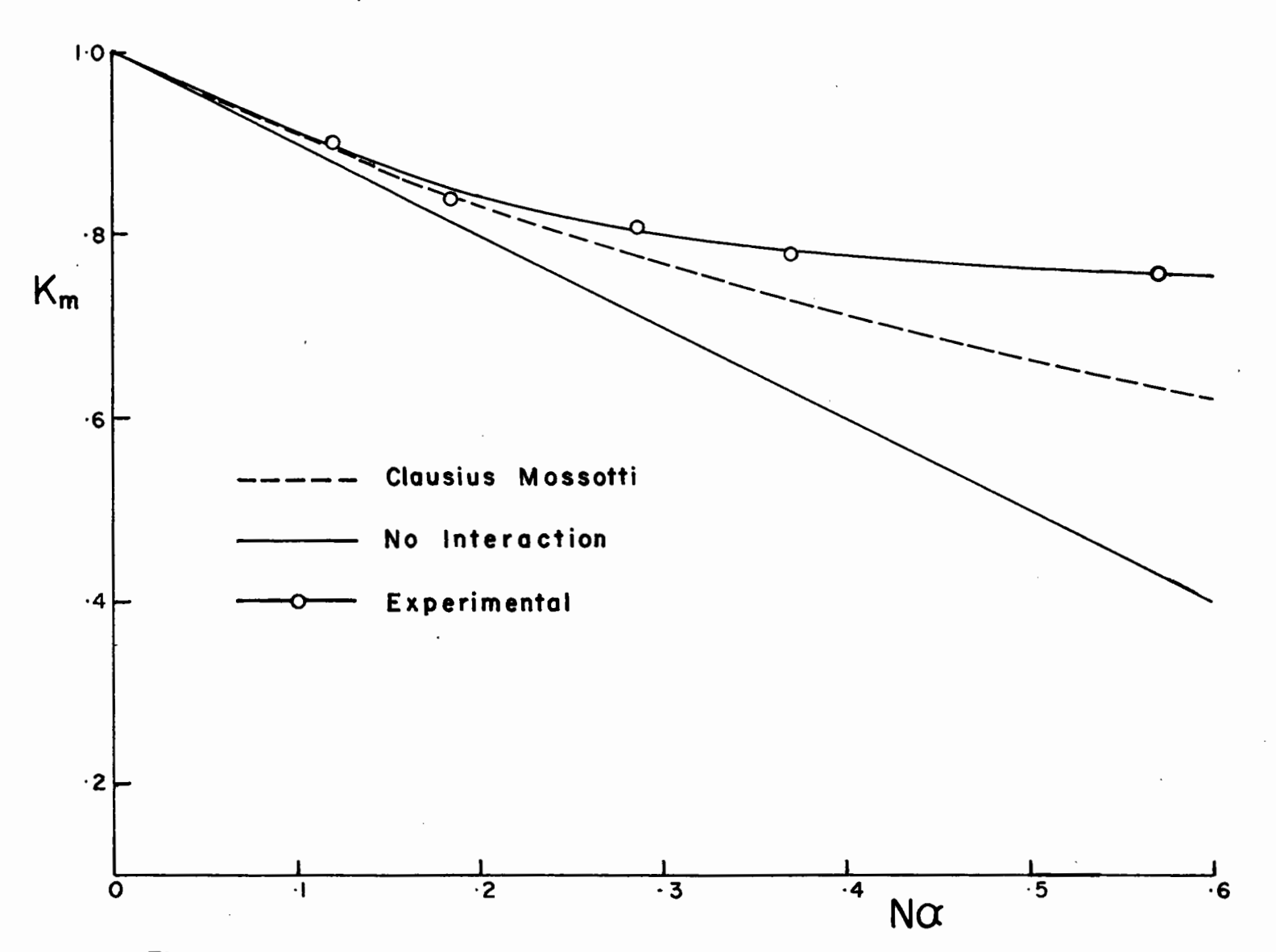


Figure 14. The permeability of aluminum disc arrays as a function of $N\alpha_{m} \boldsymbol{\cdot}$

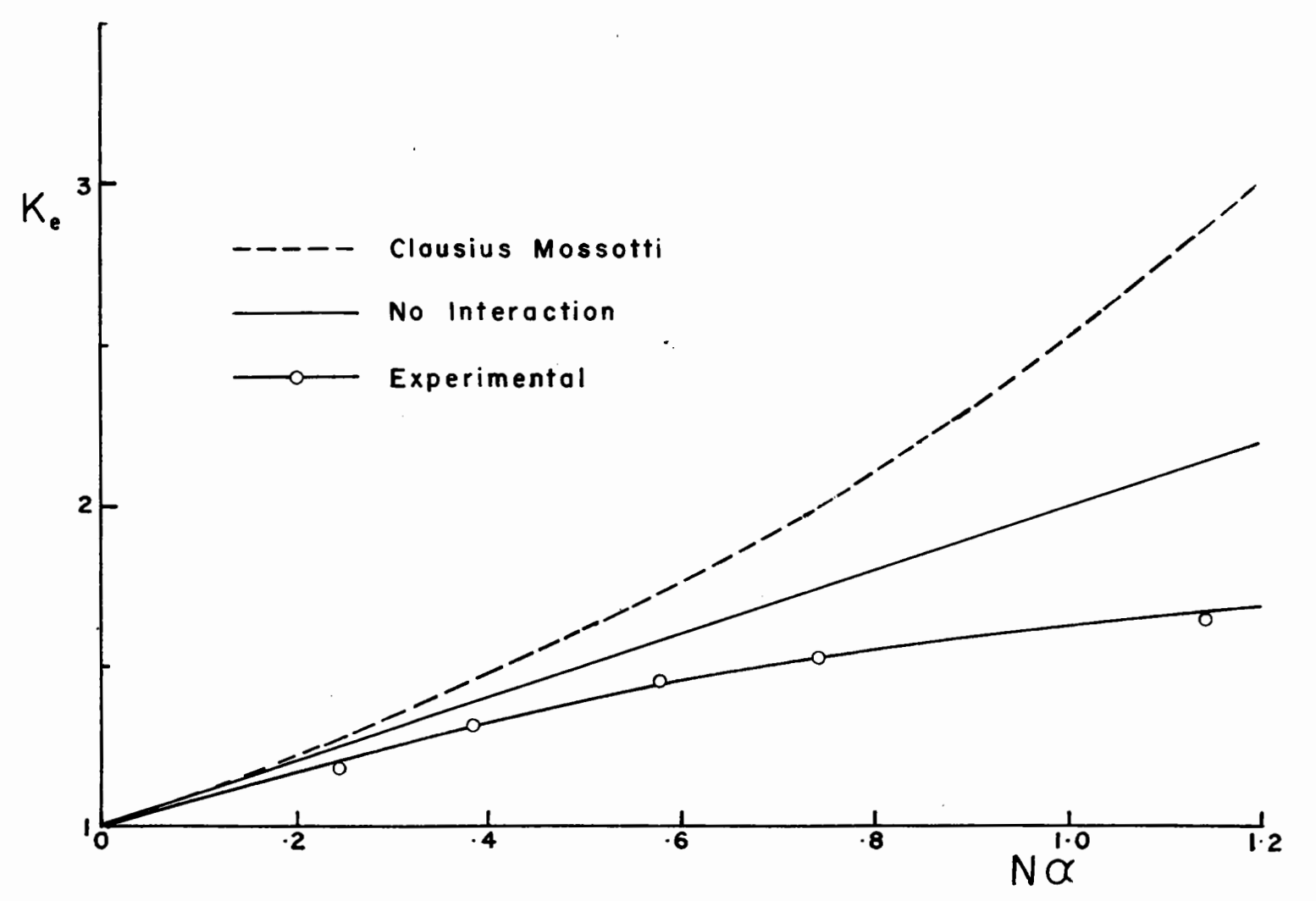


Figure 15. The dielectric constant of aluminum disc arrays as a function of $N\alpha_{\mathbf{e}}$.



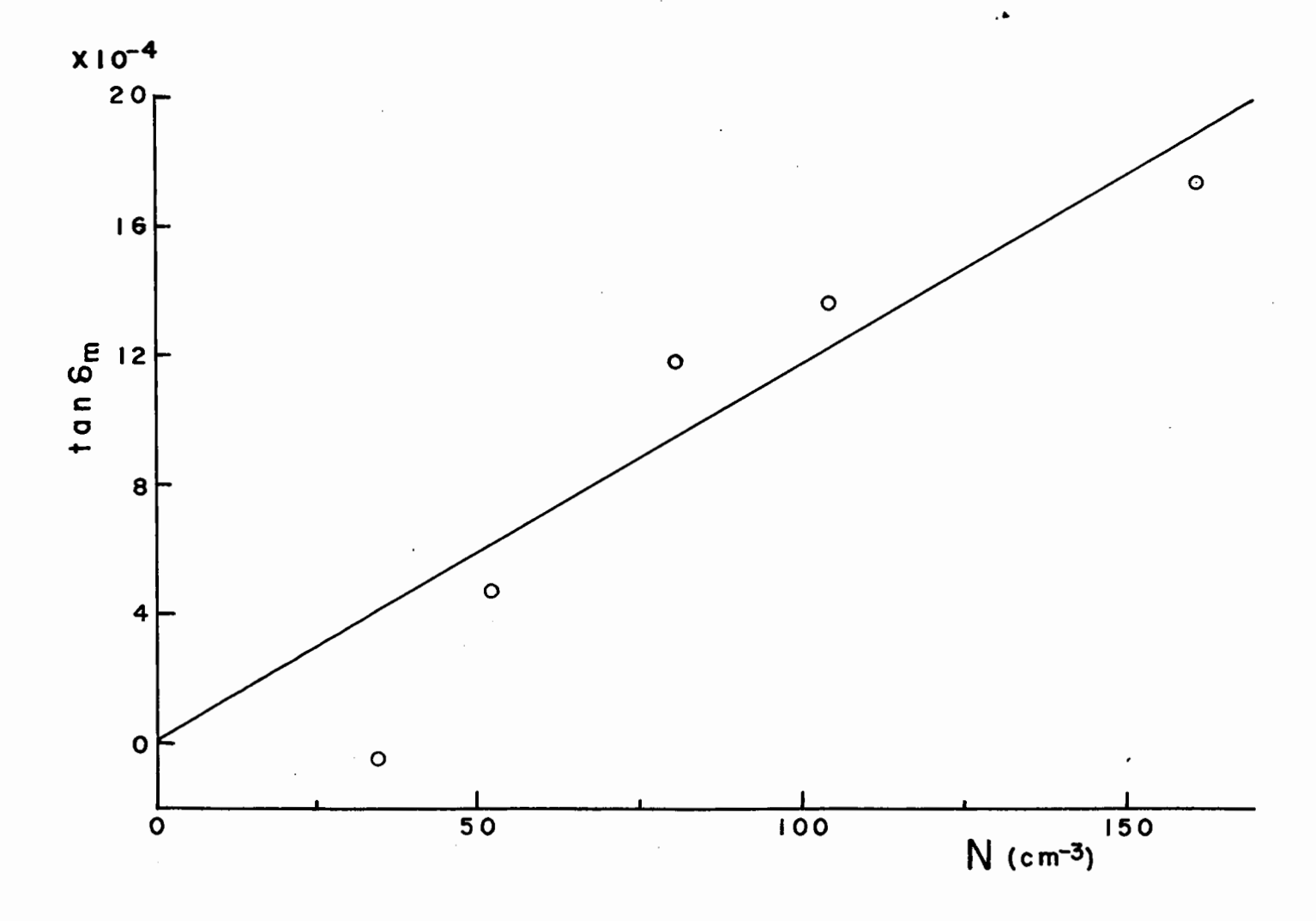


Figure 16. The measured magnetic loss tangents of aluminum disc arrays as a function of the number of particles per cm3.

it was found that at dense packing the dielectric constant was lower and the permeability higher than the corresponding quantities given by the ordinary equation. Hence, in this way the modified equation is in qualitative agreement with experiment. However, the agreement is no better than this. This is evident from the values given by the modified equation for a spacing of .1 cm. The structure constant, A_Z, is - 140.6 and the calculated dielectric constant and permeability are 1.327 and .860 respectively. These values do not agree with experiment (see Figures 11 and 12). This disagreement results from applying the modified equation to an array for which the radius of the disc is comparable with the spacing. When this is the case the interaction is such that the current and charge displacement on a disc cannot be adequately represented by magnetic and electric dipoles respectively.

The loss tangents are also plotted against disc separation in Figure 13. The electric loss tangent is small and does not vary appreciably with disc separation. This small loss tangent could possibly be due to the impurities introduced in the handling of the polystyrene spacers. The magnetic loss tangent increases as the disc separation is decreased.

Plots of the dependence of the electric and magnetic parameters on the number of particles per unit volume are given in Figures 14, 15, and 16. This is done to facilitate comparison with the more familiar methods of plotting the theoretical curves.

Chapter 6

Conclusions

It was possible to show in a quantitative manner that the diamagnetic effect associated with comparatively thick flake-shaped metallic particles randomly positioned in a wax medium is smaller than existing theories predict. This was done by comparing the experimental and theoretical values of certain quantities which according to the theory are independent of the distribution in size of the particles. It should be pointed out, however, that to get the theoretical values it was assumed that all particles were of circular contour. If the particles in general have a more elongated contour the agreement between experiment and theory is better. These considerations indicate that Carruthers qualitative explanation of permeabilities only slightly less than unity, which applies to particles with thicknesses of the order of skin depth, is not complete.

The experimental values of the loss tangents of these samples also indicate that the greater part of the total loss is associated with the circulating currents. This is in agreement with results obtained by E.I..Vogan from measurements made on fine aluminum powders.

The controlled experiments on the aluminum disc arrays gave results which point to the chief reasons for the small diamagnetism observed in the aluminum powder samples. The agreement between experiment and theory for the sparsely packed disc array in a wax supporting medium made it possible to conclude that the expression for the magnetic polarizability is correct. That is, the polarizability of a disc is essentially a real quantity(-8/3 R³), being very little effected by the finite conductivity of aluminum. Also, the results of the investigation of the densely packed arrays show that the diamagnetic permeability is much closer to unity than

- 85 -

predicted by the No-interaction or the unmodified Clausius-Mossotti equations. The smallest permeability measured is about .75 and from the graph drawn in Figure 11, it is not possible that it could be much smaller than this for more densely packed arrays. It was shown that these findings are in qualitative agreement with the Clausius-Mossotti equation modified to include the effect of the noncubic structure of the lattice.

The results of this investigation of the ordered arrays presents a possible explanation of the small diamagnetic effect contributed by the aluminum particles of approximately circular contour, the slight effect being due to interaction. That part of the diamagnetism due to the more elongated particles is small because of the small polarizabilities associated with such particles.

The values obtained from the measurement of the loss tangents of the disc arrays show that the magnetic losses increase with the number of discs, whereas the electric loss is small and almost independent of the number of discs. Because of the errors involved, the plot of the measured value of tand gave little indication of the explicit relation between tand m and the number of particles.

The experimental values of the dielectric constants of the densely packed disc arrays are much lower than the simple theories predict. This is in agreement with static measurements made by S.B.Cohn by the electrolytic tank method. These values are also in qualitative agreement with the modified Clausius-Mossotti equation. Because of this result, the explanation of comparatively large refractive indices which can be obtained with the aluminum powder dielectric is not immediately evident. However, a reasonable explanation follows from a consideration of the shape of the flake particles. Microphotographs of the particles taken by E.L. Vogan indicate that the disc contour is in general very irregular with comparatively few contours being

circular. The majority of the larger particles are elongated. This is to be expected from a consideration of the sifting process previously discussed. The electric polarizabilities of these elongated particles are much greater than their magnetic polarizabilities and hence they are more effective in producing the high refractive indices.

The Short circuit - Open circuit method of measuring dielectric parameters was enlarged in scope by making use of expressions for the propagation constants and characteristic wave impedances of certain anisotropic media in rectangular waveguide. This was done through the use of Generalized Telegraphists Equations developed by Schelkunoff. A similar treatment of the most general anisotropic media, if possible, would be extremely complicated and from a practical standpoint would be useless. However, it is possible that the theory could be applied to certain anisotropic media of practical interest, for example a gyromagnetic medium.

Because of certain simplifications in the formulae used in the numerical calculations of the Short circuit - Open circuit technique, it was possible to give a practical procedure for estimating possible errors in the measured parameters. With this procedure unusual experimental results obtained by this and other authors were explained.

Annendix A

In order to effect the inversion

$$tenh^{-1}\left(\sqrt{\frac{S^{I}}{S^{II}}} \exp\left(j\frac{T^{I}-T^{II}}{2}\right)\right) \qquad \dots (1)$$

it is first convenient to write

$$\sqrt{\frac{S^{I}}{S^{II}}} \exp \left(j \frac{T^{I} - T^{II}}{2}\right) = u + j v$$

and hence equation (1) becomes

$$tanh^{-1} (u + jv) = a + j b$$

The problem is then reduced to finding a and b if given u and v.

Equation (1) can be written in the following way:-

$$tarh(a + ib) = u + iv$$

$$= \frac{\tanh a + \tanh j b}{1 + \tanh a \tanh j b}$$

and since tanh j b = j tan b

$$u + j v = \frac{\tanh a + j \tan b}{1 + j \tanh a \tan b}$$

$$= \frac{\tanh a + i \tan b}{2} (1 - j \tanh a \tan b)$$

$$1 + \tanh a \tan^2 b$$

$$= \frac{\tanh a + \tanh a \tan^2 b}{1 + \tanh^2 a \tan^2 b} + j \frac{\tan b - \tanh^2 a \tan b}{1 + \tanh^2 a \tan^2 b}$$

$$= \frac{\tanh a (1 + \tan^2 b)}{1 + \tanh^2 a \tan^2 b} + j \frac{\tan b (1 - \tanh^2 a)}{1 + \tanh^2 a \tan^2 b}.$$

...(2)

Equation (3:3:17) shows that θ is of the order of one-half the total loss of the dielectric since $\frac{\lambda^2}{\lambda_c^2 \; k_e k_m}$ is small compared to one.

Put θ is related to a and b by the expression $\theta = \frac{a}{b}$. Thus $\frac{a}{b}$ is of the order of one-half the total loss tangent and a is of the order of $\frac{b}{2}$ tan'. For a sample one and one-eighth wavelengths long $\frac{2\pi d}{2}$ is approximately 7 and a is of the order of 3.5 $2 \tan b$ and hence $\frac{2\pi d}{3}$ is approximately. Since $\tan a = a - \frac{a^3}{3} + \frac{2a^5}{15} - \cdots$, equation (2) may be written

$$u + j v = \frac{a(1 + \tan^2 b)}{1 + \tanh^2 a \tan^2 b} + j \frac{\tan b}{1 + \tanh^2 a \tan^2 b} \cdot ...(3)$$

Also, if the measurement is made for a sample length near an odd multiple of one-eighth of a wavelength, tan b = 1 and $\tanh^2 a \tan^2 b \ll 1$ and equation (3) becomes

$$u + j v = a(1 + tan^2b) + j tan b$$

from which the relations

$$b = \tan^{-1}v \qquad \qquad \cdots (4)$$

and
$$a = \frac{u}{1 + v^2}$$
 ...(5

are evident. Previous to this investigation a and b have been determined by the rigorous formulae

$$b = \tan^{-1} \left(\frac{1 - u^2 - v^2}{2v} \pm \sqrt{1 + (\frac{1 - u^2 - v^2}{2v})} \right) \dots (6)$$

$$\cosh a = \sqrt{\frac{\sin b \cos b}{v} + \sin^2 b} ...(7)$$

This method of getting b is straight forward but long. The term on the right hand of equation (7) must be very little greater than one since a is small. Thus in order to get accurate values of a, cos b and sin b had to be accurately known. In fact, values extrapolated in cos and sin tables of arguments to the nearest one-thousandth of a radian had to be used.

The errors involved in such a procedure might easily be greater than the error due to the use of the approximate relation given in equation (5). For example, consider a sample for which $\Sigma \tan \delta = .0340$ and $\tanh(a+jb)=.1580 + jl.0681$, .1580 and 1.0681 being actual measured values of u and v respectively. By equations (6) and (7)

$$a = .0733$$

$$b = 3.9657$$

and by the approximate equations

$$a = .0738$$

$$b = 3.9599.$$

However, a and b can be determined more accurately by substituting these latter approximate values into the right hand side of the equations

$$tanh a = \frac{u(1 + tanh^2 a tan^2 b)}{1 + tan^2 b}$$

$$\tan b = \frac{v(1 + \tanh^2 a \tan^2 b)}{1 - \tanh^2 a}$$

thus giving

$$a = .0744$$

$$b = 3.9657$$

Hence it is seen that the value of a obtained by equations (6) and (7) is about 1.5% lower than the true value.

On the following page a typical calculation is carried out from measurements made on a lucite sample. The term $(n_a^i - n_s^i) \stackrel{\triangle}{\longrightarrow} 2$ accounts for the effect of the slot of the detecting section on the position of the minimum and the second term in the expression for $\triangle X$ serves to correct for the losses in the guide walls⁴. The equations appearing on this calculation sheet will be used in the discussion of errors in Appendix B.

Calculation Sheet for Short circuit - Open circuit Measurement of Isotropic Dielectrics

	of Isotropic Dielectric	S
Sample: Lucite	$\lambda_{go} = 4.4705$	$k_e = 2.589$
Run: 7	Date= 6th January 1953	$k_{\rm m} = 1.0086$
$\lambda_{\mathbf{c}} = 4.5822$	Temp= 20°C	$tanb_e = .0104$
$\Delta \lambda = .0270$, Thic	kness= 1.3698	$tanb_{m} =0024$
$X = (N_{S}-N_{S}$	$(x + \frac{n_{s}\lambda_{go}}{2}) \frac{\lambda_{go}}{n_{a}\lambda_{go}} + (n_{a}^{1} - \frac{n_{s}\lambda_{go}}{2})$	$n_s!$) $\frac{\Delta \lambda}{2} - d - \left(\frac{\lambda_{go}}{4}\right)$
λ_{go} = 4.4705 ΔX_a =2.5141 ΔX_a = 2.5141 $\frac{2.5093}{0.0048}$ = $\frac{2.5095}{0.0046}$	$\lambda_{go} = 4.4705$ $\Delta X_{s}^{I} = 1.3266 \Delta X_{s}^{I} = 1.3270$ $\frac{1.3054}{0.0012} = \frac{1.3057}{0.0013}$	$\lambda_{go} = 4.4705$ $\Delta X_{s}^{II} = .8631 \Delta X_{s}^{II} = .8630$ $\frac{.8367}{.0264} = .0268$
$N_a = 2.5188$	$N_{\rm S}^{\rm I} = 1.3162$	$N_{s}^{II} = .8497$
$\frac{2\Delta X_{a}}{n_{a}\lambda_{g0}} \cdot 00042$	$(n_a'-n_s')^{\perp} \frac{4\lambda}{2} = .0073$	$(n_a^i - n_s^i)^{\frac{11}{2}} = .0096$
I Sample at short	II Sample λ_{go}	/4 from short
① $x^{I} = 1.9122$		12
② $\Delta x^{I} = .0176$		
		848
$4 \tan \frac{2\pi X^{I}}{\lambda_{go}} = \tan 2.6875$	$=4881 \text{(4)} \tan \frac{2\pi x^{\text{II}}}{\lambda_{go}}$	= tan .4655 = .5023
	3 (3) ² + ($(4)^2)^{1/2} = .5026$
$6 \tan^{-1} 4 / 3 = \tan^{-1} -3$		
$7 \tan^{-1} 3x4 =0060$	7 tan ⁻¹ 3 x	(4) = .00928
$ (1 + 3^2 x 4^2)^{1/2} = $	8 (1 + 3)2	$(x \oplus 2)^{1/2} = 1$
7 $\tan^{-1}(3)x(4) =0060$ 8 $(1 + (3)^2x(4)^2)^{1/2} = 1$ 9 $\sin^{-1}(3)x(4) =0060$ 9 $\sin^{-1}(3)x(4) =0060$	-⑥+⑦) ⑤ S ^Ⅲ exp(jT	$^{II}) = \overset{(5)}{\underbrace{8}} \exp \ \mathbf{j}(-\underbrace{6} + 7)$

 $= .5026 \exp(-j 1.5247)$

 $= .4883 \exp(j 1.5394)$

(10)
$$\frac{Z_{ki}}{Z_{ko}} = \sqrt{S^{I}S^{II}} \exp j \frac{T^{I} + T^{II}}{2} = B \exp(j\emptyset) = .4954 \exp(j .00732)$$

(1)
$$\tanh \gamma_{id} = \tanh(a + j b) = \sqrt{\frac{S^{I} \exp(jT^{I})}{S^{II} \exp(jT^{II})}} = u + j v = .0382 + j .9849$$

(12)
$$b = \tan^{-1} v + m\pi = .7778 + \pi = 3.9194$$

(3)
$$a = \frac{u}{1+v^2} = .0194$$

$$\frac{\gamma_{i}}{\gamma_{0}} = \frac{\sqrt{b^{2} + \epsilon^{2}}}{\frac{2\pi d}{\lambda_{g0}}} \exp(-j \tan^{-1} \frac{a}{b}) = A \exp(-j\theta) = 2.0359 \exp(-j .00495)$$

15
$$tanb_m = -tan(\emptyset-9) = -.00237$$

(16)
$$k_m = \frac{AB}{\sqrt{1 + \tan^2 \delta_m}} = 1.0086$$

(17)
$$k_e k_m = \frac{\chi^2}{\lambda_{go}^2} \left(A^2 + \frac{\lambda_{go}^2}{\lambda_c^2} \right) = 2.6115$$

(13)
$$\Sigma \tanh = 20 \left(1 - \frac{\lambda^2}{\lambda_0^2} \frac{1}{k_0 k_m}\right) = .00805$$

(19)
$$k_e = (19) = 2.5892$$

20
$$tanb_e = 18 - 15 = .01042$$

Appendix B

In the following analysis of the errors in the Short circuit-Open circuit measurement, it is assumed that the experimental error associated with the measurement of λ_{go} is negligible. This is a valid assumption in view of the precision of the microwave components involved in such a measurement.

The individual steps in the procedure are not explained in detail since they involve simple differentiations and approximations based on the assumption that the electric and magnetic loss tangents are small. Also, the steps are numbered to correspond to those in the calculation sheet given in Appendix A.

A δ preceding a symbol refers to the algebraic value of the experimental error associated with the quantity represented by that symbol. No confusion should arise between this δ and those associated with the electromagnetic attenuation in the dielectric samples.

Calculation Procedure for the Estimation of Errors

and 2 The errors in X and AX are estimated in the usual manner by considering the precision of the instruments involved.

8 Negligible error

$$\delta T = -\delta + \delta T$$

$$\delta B = \delta \sqrt{S^{I}S^{II}} = \frac{B}{2} \left[\frac{\delta S^{I}}{S^{I}} + \frac{\delta S^{II}}{S^{II}} \right], \quad \delta \emptyset = \frac{1}{2} \left(\delta T^{I} + \delta T^{II} \right)$$

(1) Since
$$u = \sqrt{\frac{S^{I}}{S^{II}}} \left[\frac{\pi}{2} - \frac{T^{I} - T^{II}}{2} \right]$$
 and $v = \sqrt{\frac{S^{I}}{S^{II}}}$

$$\delta \mathbf{u} = \frac{\mathbf{v}}{2} (\delta \mathbf{T}^{\mathbf{I}} - \delta \mathbf{T}^{\mathbf{I}})$$
and
$$\delta \mathbf{v} = \frac{1}{2B} (\delta \mathbf{S}^{\mathbf{I}} - \mathbf{v}^2 \delta \mathbf{S}^{\mathbf{II}})$$

12
$$\delta b = \frac{1}{1+v^2} \delta v$$

= $\frac{1}{2B(1+v^2)} (\delta S^{I} - v^2 \delta S^{II})$

Since
$$A = \frac{b\lambda_{go}}{2\pi d}$$

$$bA = \frac{\lambda_{go}}{2\pi d} bb - \frac{b\lambda_{go}}{2\pi d^2} bd.$$
Also since $\theta = -a/b$

$$\delta\theta = -\frac{\delta a}{b} + \frac{a\delta b}{b^2}.$$

The calculation procedure up to this point is the same for either isotropic or anisotropic media. The errors in the electric and magnetic parameters can easily be obtained by making use of the relations between $k_e, k_m, tanbe$, tanbm and A, B, Θ , \emptyset which are pertinent to the media under consideration.

With this outline it is not difficult to estimate the errors in the parameters of a sample after a measurement has been made and the values of the parameters obtained. If the estimated errors for a sample to be measured, for which approximate values of the parameters are known, are needed, considerably more numerical work is required. That is, the calculation procedure outlined in Appendix A must be inverted so that approximate values of X^{I} , X^{II} , ΔX^{I} and ΔX^{II} may be obtained from the known dielectric parameters. This was done to obtain the plots given in Chapter 4. It should be mentioned that this inversion process is comparatively simple if the proposed measurement is to be made for a sample with a length which is close to an odd multiple of one-eighth of a wavelength.

Bibliography

- 1 W. E. Kock, Proc. I.R.E., 34, 828, Nov. 1946.
- 2 W. E. Kock, B.S.T.J., 27, 58-82, Jan. 1948.
- J. A. Carruthers, Eaton Electronics Research Laboratory, McGill University. Report, U.S.A.F., Contract AF 19(122)-81, Oct. 1951.
- 4 E. L. Vogan, Eaton Electronics Research Laboratory, McGill
 University. Report No. 6, U.S.A.F., Contract AF 19(122)-81,
 April 1952.
- 5 W. B. Westphal, Technical Report XXXVI, Laboratory for Insulation Research, M.I.T.
- 6 N. M. Rust, J. Instn. El. Eng., 93(IIIA), 50-51, 1946.
- 7 0. M. Stuetzer, Proc. 1.R.E., 38, 1053-1056, 1950.
- 8 R. W. Corkum, Air Force Cambridge Research Laboratories, Report E 5068, March 1951.
- 9 C. Susskind, Final Report, U.S.A.F. Contract No. AF 19(122)-270,

 June 1951.
- 10 G. Estrin, Proc. I.R.E., 39, 821-826, July 1951.
- 11 H..E. J. Neugebauer, Eaton Electronics Research Laboratory, McGill
 University. Report No. 19, U.S.A.F. Contract AF 19(122)-81,
 April 1952.
- 12 G. Estrin, J. Appl. Phys., 21, 667-670, 1950
- 13 H. E. J. Neugebauer, Eaton Electronics Research Laboratory, McGill University. U.S.A.F. Report No. 20, Contract AF 19(122)-81,

 April 1952.
- 14 L. Lewin, J. Instn. El. Eng., 94(III), 65-68, 1947.
- 15 S. B. Cohn, J. Appl. Phys., 20, 257-262 and 1011, 1949.

- 16 H. S. Bennett, J. Appl. Phys., <u>24</u>, 785-810, **1**953.
 - C. Flammer, Phys. Rev., <u>89</u>, 1298, 1953.
 - D. Slepian, Project V-7, Research Staff, Harvard University
- 17 C. Flammer, McGill University Symposium on Microwave Optics,
 Paper No. 29, June 1953. To be published in Can. J. Phys.
- 18 J. C. Slater, Phys. Rev., 45, 794, 1934.
- 19 S. A. Schelkunoff, Bell System Tech. J. XXXI, 784-801, July 1952.
- 20 S. A. Schelkunoff, <u>Electromagnetic Waves</u>, New York: D. Van Nostrand Company, Inc., 1943.
- 21 Ramo and Whinnery, <u>Fields and Waves in Modern Radio</u>, New York:

 John Wiley and Sons, Inc., 1952.
- 22 J. M. Kelly, J. O. Stenoien and D. E. Isbell, J. Appl. Phys. 24, 258, March 1953.